The Thesis Committee for Brandon Emil Boor
Certifies that this is the approved version of the following thesis:

Monolayer & Multilayer Particle Resuspension from Indoor Surfaces: Literature Review and Experimental Methodology

APPROVED BY
SUPERVISING COMMITTEE:

Supervisor:

Atila Novoselac

Jeffrey A. Siegel

Monolayer & Multilayer Particle Resuspension from Indoor Surfaces: Literature Review and Experimental Methodology

by

Brandon Emil Boor, B.S.

Thesis

Presented to the Faculty of the Graduate School of

The University of Texas at Austin

in Partial Fulfillment

of the Requirements

for the Degree of

Master of Science in Engineering

The University of Texas at Austin

December 2010

Dedication

To my mom, dad, and sister

Acknowledgements

I would like to sincerely thank my research advisor Dr. Atila Novoselac for his continued guidance and support. His hands-on and practical approach to research and engineering has taught me a lot about how to solve problems in the laboratory and improve my experimental methods. I would also like to thank Dr. Jeffrey Siegel for providing additional technical guidance and support. I would like to acknowledge Dr. Angela Bardo and the Microscopy and Imaging Facility of the Institute for Cellular and Molecular Biology for providing training and access to the fluorescence stereomicroscope used in this research. Lastly, I would like to thank my family for their love and support.

December 2010

Abstract

Monolayer & Multilayer Particle Resuspension from Indoor Surfaces: Literature Review and Experimental Methodology

Brandon Emil Boor, M.S.E

The University of Texas at Austin, 2010

Supervisor: Atila Novoselac

Resuspension is an important source of particles in the indoor environment. A variable that may have a significant impact on the fraction of particles removed from indoor surfaces is the type of particle deposit. Particles may be deposited in either a monolayer, where there is minimal particle-to-particle contact, or a multilayer, where there is substantial particle-to-particle contact and interaction. This paper provides a review of theoretical and experimental studies on particle resuspension from monolayer and multilayer particle deposits. In addition, an experimental methodology was developed to determine resuspension from the two types of deposits on indoor surfaces. Seeded samples were exposed to controlled flow conditions in a micro-scale wind tunnel and were analyzed with fluorescence stereomicroscopy. Resuspension was found to occur at significantly lower velocities for multilayer deposits compared to monolayer deposits.

Table of Contents

List of Tables

List of Figures

List of Illustrations

Chapter 1: Introduction

It has become increasingly important to characterize the sources of indoor air pollution because people spend greater than 87% of their time indoors (Klepeis et al. 2001). A class of indoor air pollutants, inhalable coarse particles, has attracted considerable attention in the indoor air literature because of the deleterious health effects associated with human inhalation exposure. According to the U.S. Environmental Protection Agency (EPA), inhalable coarse particles are defined as particles with diameters ranging from 2.5 μm ($PM_{2.5}$) to 10 μm (PM_{10}) (EPA, PM Standards Revision – 2006). Epidemiological studies suggest that elevated airborne concentrations of $PM_{2.5}$-PM_{10} are associated with an increased risk of cardiovascular disease (Pope et al. 1999, Peters et al. 2000, Polichetti et al. 2009), lung inflammation (Souza et al. 1998), and an increase in mortality (Ostro et al. 1998).

Sources of particles in the indoor environment include particles of outdoor origin and particles generated indoors from a variety of sources. Particles may be transported from outdoor air via mechanical and natural ventilation and infiltration (e.g. Nazaroff 2004) and can be generated indoors through cooking and smoking (e.g. Wallace 1996), among other sources. As the particles are transported throughout the air via ventilation, buoyancy driven airflow, mechanical fans, and human movement, they will eventually deposit on indoor surfaces, including floors, walls, and ventilation ducts. Although deposition acts as a removal mechanism for particles, thereby reducing airborne concentrations, deposited particles are still viable to become airborne again through a process known as resuspension (also referred to as reaerosolization or re-entrainment).

Resuspension is considered a secondary source of particles and is primarily associated with particles in the inhalable coarse size range (2.5 to 10 μm) in the indoor

environment. Resuspension has received attention in the scientific literature for nearly half a century, beginning with Bangold 1941 in his study of wind-induced disturbance of sand dunes and continuing with Corn 1961 and Corn and Stein 1965 in their fundamental studies of particle adhesion and detachment. Sehmel 1980 and Nicholson 1988 provided reviews of the existing resuspension literature at time, which primarily focused on soil particle transport, wind erosion, and the transport of contaminated particles generated from nuclear weapon tests and accidental releases from nuclear reactors. The later received attention when it was discovered that the resuspension of deposited particles could explain how decontaminated regions regained radioactivity after the Chernobyl disaster in 1986 (Nicholson 1988). Resuspension in the outdoor environment was also a concern because of the potential transport of pesticides and fungal spores amongst crops. It was not until the recent studies by Thatcher and Layton 1995, Batterman and Burge 1996, and Ferro et al. 2004 that resuspension was considered as a potential secondary source of particles in the indoor environment, where people spend the majority of their time and are at risk for inhalation exposure.

Resuspension in the indoor environment can be an exposure pathway to the multitude of pollutants that are commonly found in indoor house dust. Some of these pollutants include: allergens (e.g. Swanson et al. 1985, O'Meara and Tovey 2000), polycyclic aromatic hydrocarbons, and semi-volatile organic compounds such as phthalates and brominated flame retardants (e.g. Ott et al. 2005).

Thatcher and Layton 1995 observed that resuspension significantly increased airborne particle concentrations in a home and additional studies, e.g. Ferro et al. 2004, Qian & Ferro 2008, Rosati et al. 2008, have linked resuspension with human activities indoors, such as walking and folding blankets. Furthermore, several studies have demonstrated that resuspension in ventilation systems can be a potential secondary source

of particles indoors (e.g. Batterman and Burge 1996, Sippola and Nazaroff 2004, and Krauter and Biermann 2007).

Resuspension likely contributes to the so-called "personal cloud effect" or "Pig-pen effect," in which personal exposures of 10 μm particles tend to be greater than either indoor or outdoor concentrations (Wallace 1996). As occupants engage in various dust disturbing activities throughout their home, resuspended particles can be transported to their breathing zone via their thermal plumes, thereby increasing their personal exposure (Rim and Novoselac 2009).

In the indoor environment, many variables can impact the number of particles resuspended from a surface, and ultimately the amount of particles occupants can be exposed to. To understand the relationship between particle characteristics, environmental conditions, and resuspension, this paper presents an experimental methodology to determine resuspension of inhalable coarse particles from indoor surfaces. The methodology builds upon established methods for empirically determining the number of particles resuspended for a given set of experimental conditions and previous resuspension research conducted at The University of Texas at Austin (Lohaus et al. 2008, Mukai et al. 2009).

The focus of this research is on the aerodynamic removal of particles, where the dominant removal forces acting on a deposited particle are lift and drag (discussed in further detail in Chapter 2). In the indoor environment, aerodynamic forces are the primary removal mechanisms for the resuspension of particles by walking, as discussed in such papers as Gomes et al. 2007, and the resuspension of particles in ventilation systems, e.g. Krauter and Biermann 2007. Other removal mechanisms also resuspend particles, including mechanical forces such as abrasion or vibration; however, these forces were not investigated in this study.

This study examines two types of particle deposits that represent the potential spectrum of diverse particle deposits in the indoor environment: a monolayer deposit and a multilayer deposit. A monolayer deposit is one in which particles are sparsely deposited on a surface and there is minimal to no contact between them. This deposit has predominately been the focus of fundamental resuspension research since it provides a means to examine the interaction between a particle and the surface it is in contact with. A multilayer deposit is defined as a porous structure of particles deposited on top of one another, forming multiple layers where the is substantial particle-to-particle contact. The dynamics of particle adhesion and resuspension are considerably different for multilayer deposits. Adhesion between particles is less than that between a particle and a surface, as discussed in Lazaridis and Drossinos 1998. Furthermore, the fluid dynamics become more complex due to flow above and within the porous structure, which likely generates different aerodynamic removal forces.

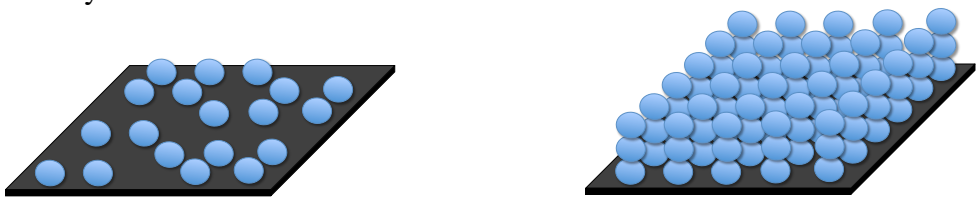

Illustration 1.1: Monolayer (left) and multilayer (right) particle deposits

The structure of particle deposits in the indoor environment has not been thoroughly examined to date, so it is difficult to make conclusions about which type of deposit is more prevalent on indoor surfaces. However, it is reasonable to assume real deposits fall somewhere between a pure, sparse monolayer and a multilayer. Visible dust accumulations on the floor or on the surface of a ventilation duct are likely multilayer deposits or deposits of particle clusters, whereas a monolayer deposit likely exists on top of recently cleaned surfaces. This study examined both deposits to provide upper and

lower bounds on particle resuspension in an attempt to demonstrate the significance of this variable on resuspension. This will aid in our understanding of secondary sources of inhalable coarse particles in the indoor environment and provide justification for future work on the topic.

This research is described in detail in the following chapters in the following manner: the second chapter provides a review of extant literature pertaining to particle adhesion and resuspension, from both theoretical and experimental perspectives. The third chapter presents the experimental methodology developed, with a detailed summary of the various stages comprising the method. The fourth chapter gives the results for resuspension from monolayer and multilayer deposits and a brief discussion of each. The fifth chapter summarizes the research and discusses ongoing and future work related to the topic. Additional information is provided in the appendix and a complete reference list is included.

Chapter 2: Literature Review

This chapter begins with a discussion on particle adhesion and continues with summaries of monolayer and multilayer particle resuspension models. Fundamental experimental studies on aerodynamic particle resuspension from the two types of deposits are also discussed.

2.1 Particle Adhesion Models

Adhesion forces must be overcome for a deposited particle to resuspend and become airborne. It is well established in the literature that three primary adhesive forces exist between a particle and the surface it is in contact with: van der Waals, electrostatic, and capillary. These adhesion forces are considered in many of the resuspension models discussed in Section 2.2.

2.1.1 Van der Waals Force

Van der Waals forces, which are the long-range attractive forces that exist between molecules, arise from molecular dipoles. All atoms experience constant vibrational motion, which distorts the symmetric spatial distribution of electrons with respect to the nucleus. This in turn creates small, localized regions of concentrated charge. These dipoles then induce a distortion of the electrical symmetry of an adjacent molecule, creating a second dipole and a resulting weak attractive force between the two (Hinds 1999, Callister 2007). Because both the surface and particle exhibit surface roughness in the form of asperities (on the order of nanometers), the two are separated by some distance, x. With time, this separation distance is reduced and the contact area increases, a process known as flattening (Tsai 1991). Flattening is a function of the hardness of the particle and surface material, and generally is reduced as hardness

increases. As presented in Hinds 1999, the van der Waals force can be calculated from the following relationship:

$$F_{adh,vdW} = \frac{A_{132} d_p}{12x^2} \quad (1)$$

Where A_{132} is known as the Hamaker constant and d_p is the particle diameter. The Hamaker constant depends on the two materials involved and the surrounding medium that separates them. Kim et al. 2010 provides an additional relationship required to derive Hamaker constants:

$$A_{132} \cong (\sqrt{A_{11}} - \sqrt{A_{33}})(\sqrt{A_{22}} - \sqrt{A_{33}}) \quad (2)$$

Where the particle is represented by *1*, the surface by *2*, and the separating medium by *3* and *A* is the Hamaker constant. Typical values for common materials have been found to range between 6 to 150 x 10^{-20} J. In their study of particle detachment from vinyl and rubber tile, Hu et al. 2008 assumed a value of 10 x 10^{-20} J. Values for steel, glass, and latex particle-surface interactions can be found in Kim et al. 2010, however, a comprehensive database of Hamaker constants for real indoor surfaces and particles is very limited, and thus approximations are often used.

2.1.2 Electrostatic Force

As a particle is transported through the indoor environment, it may acquire a net electric charge. There are a variety of mechanisms by which a particle can accumulate a charge, including static electrification via mechanical abrasion, diffusion charging due the random collisions of air ions with the particle, and field charging if a strong electric field is present, explained in detail by Hinds 1999. The total amount of charge carried by a particle is determined as follows:

$$q = ne \quad (3)$$

Where q it the total electrical charge, n is the unit of charge, and e is the elementary unit of charge, 1.6 x 10^{-19} coulombs (C). The average number of absolute charges on a particle can be determined by the following empirical relation, which for particles greater than 0.2 μm in diameter, is accurate to within ±5%:

$$\bar{n} \approx 2.37 d_p^{0.5} \tag{4}$$

Eventually, as neutral particles acquire a charge and charged particles attract oppositely charged ions, particles will tend toward the Boltzmann equilibrium charge distribution. Additional information on determining the charge distribution can be found in Hinds 1999. According the Hays 1978, the charge carried by a particle is assumed to be concentrated on its asperities. The electrostatic adhesive force is given as (Ahmadi and Guo 2007):

$$F_{adh,elec} = qE - \frac{q^2}{16\pi\varepsilon_0 x_{ps}^2} + \frac{qEd_p^3}{16x_{ps}^3} - \frac{3\pi\varepsilon_0 d_p^6 E^2}{128 x_{ps}^4} \tag{5}$$

Where E is the applied electric field strength, ε_0 is permittivity of a vacuum, 8.85 x 10^{-12} $C^2/N\text{-}m^2$, x_{ps} is the separation distance between the center of the particle and the surface, and q is the total electrical charge. The terms on the right-hand side represent, respectively, the Coulombic force due the applied electric field, the image force, the dielectrophoretic force, and the polarization force. For typical indoor environments in which there is no applied electrical field present, E can be assumed to be zero and the above equation reduces accordingly. An alternative version that accounts for the surface roughness of the particle is presented in Ahmadi and Guo 2007. The fundamentals of electrostatic adhesion were applied to empirically determine the adhesion force between particles and common indoor materials in Hu et al. 2008, which found the empirically derived forces to generally be lower than those predicted by theoretical models.

2.1.3 Capillary Force

The last primary adhesive force is the capillary force, which is created as water vapor condenses between a particle and a surface, forming a water meniscus. The meniscus will grow until a period of equilibrium is obtained in which the rate of condensation and evaporation are equivalent (Pakarinen et al. 2005). Ahmadi et al. 2007 found that the presence of a capillary force significantly increased particle adhesion to a surface. The capillary force is the sum of the capillary pressure force, created by the negative Laplace pressure force that pulls the particle and surface together (approximately 9 x 10^7 Pa for 50% relative humidity), and the surface tension force, which is due to the surface tension that pulls the contact line of the particle and meniscus closer to that of the surface and meniscus. Pakarinen et al. 2005 presented general models for the two forces, which can be simplified based on several assumptions. The capillary pressure force for large spherical particles, where the particle radius is significantly greater than the meniscus vertical radius of curvature, can be determined as follows:

$$F_{adh,cappres} = \pi\gamma d_p\left[\cos(\theta_1) + \cos(\theta_2)\right] \tag{6}$$

Where γ is the surface tension of the condensed water vapor, 72.8 mJ/m^2 for water at 20°C, and θ_1 and θ_2 are the meniscus contact angles to the particle and to the surface, respectively. The authors assumed that the angles are equivalent and not a function of relative humidity. The surface tension force is also a function of the surface tension:

$$F_{adh,st} = l\gamma\cos(\alpha) \tag{7}$$

Where l is the perimeter of the contact between the meniscus and the particle and $\gamma cos(\alpha)$ is the vertical component of the surface tension. Pakarinen et al. 2005 assumed

this force the be small compared to the capillary pressure force for particles greater than 2 μm in diameter, thereby reducing the capillary force to:

$$F_{adh,cap} = 2\pi\gamma d_p \cos(\theta) \tag{8}$$

Where θ is the meniscus contact angle. Ahmadi et al. 2007 noted that the last parameter could be neglected for small meniscus contact, or "wetting," angles. Pakarinen et al. 2005 found that for particles greater than 2 μm in diameter, the capillary pressure force is independent of relative humidity, whereas smaller, nanoparticles experience a much stronger dependence. The presence of the water meniscus will also influence the van der Waals force by changing the separating medium from air to water vapor. As mentioned earlier, the Hamaker constant is dependent on the separating medium; if condensed water vapor is present, water-mediated Hamaker constants must be used, as done for silica and titania in Paajanen et al. 2006.

Based on the preceding theoretical analysis, the total adhesion force is the sum of the individual adhesive forces, all of which are proportional the diameter of the particle, d_p. A simple analysis comparing each individual adhesive force normalized by the particle diameter (F_{adh}/d_p) shows that the capillary force is dominant, followed by the van der Waals force, and then the electrostatic force, which tends to be very small in the absence of an electric field.

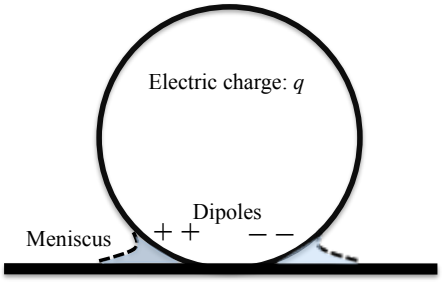

Illustration 2.1: Particle adhesion to a surface

2.1.4 Surface Energy Adhesion Models

Several popular adhesion models, widely used in many industries such as powder coating and pharmaceuticals, approach particle adhesion from the perspective of the surface energy associated with two bodies in contact. The most popular model is the Johnson-Kendall-Roberts (JKR) model, proposed by Johnson, Kendall, and Roberts in their 1971 paper. The JKR model accounts for the thermodynamic work of adhesion (surface energy per unit area), which is a function of the Hamaker constant, the separation distance at the contact site, and the elastic deformation of the particle and surface (Johnson et al. 1971). When a particle and surface are in contact with one another, the contact area takes the form of a contact circle with a radius that is dependent on the thermodynamic work of adhesion and a composite Young's modulus based on the two materials in contact. This model has been applied in various resuspension models, as discussed in Section 2.2.2. Additional adhesion models have been developed, notably the Derjaguin, Muller, and Toporov (DMT) model and the Muller, Yushchenko, and Derjaguin (MYD) model. DMT is typically used for small particles and low surface energy systems, whereas JKR is more appropriate for larger particles and high surface energy systems (Muller et al. 1980).

These models further demonstrate the importance of the properties of the two materials involved (e.g. Young's modulus) on the resulting adhesive forces, and subsequently on particle resuspension. In the indoor environment, particles and surfaces can be very diverse, so adhesion cannot be assumed constant over all particle and surface materials.

2.1.5 Effect of Relative Humidity on the Total Adhesion Force

Because the relative humidity indoors may fluctuant from one climate and/or season to another, its impact on the total adhesion force between a particle and a surface

must be discussed in further detail. As previously mentioned in Section 2.1.3, the literature suggests that the capillary force is not a function of relative humidity (for particles greater than 2 μm in diameter). However, modeling and experimental results have suggested that the total adhesion force, sometimes reported as the pull-off force, is dependent on relative humidity, and tends to increase with increasing humidity. Hinds 1999 presented an empirical relation for the total adhesive force between a particle and a flat surface that is indeed a function of relative humidity:

$$F_{adh} = 0.063 d_p \left[1 + 0.009(\beta)\right] \tag{9}$$

Where β is the relative humidity in percent. This equation is plotted in Figure 2.1, where the adhesion force has been normalized by the maximum adhesion force at 100% relative humidity. It is apparent that increasing the relative humidity from a dry, 20%, to a moist 70%, increases the adhesion by approximately 40%. This demonstrates that particle adhesion, and ultimately resuspension, may vary from one indoor environment to another.

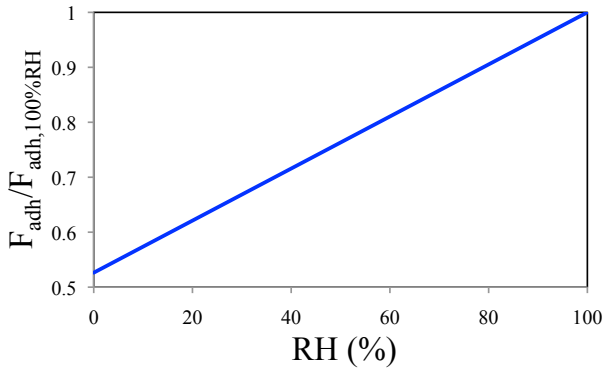

Figure 2.1: Normalized adhesion force as a function of relative humidity (RH, %)

Various studies, including Corn and Stein 1965, demonstrated the humidity dependence of adhesion, and ultimately resuspension. Particle adhesion was found to increase by roughly 50% due to increasing the relative humidity form 35 to 75%. In their adhesion model for a 70 μm particle, Nitschke and Schmidt found the adhesion force to

increase rapidly above 50% relative humidity until saturation was obtained, upon which the force suddenly dropped.

To experimentally investigate the adhesion of particles to surfaces, an atomic force microscope (AFM) is typically used. The force required to remove, or pull-off, a particle is recorded for various environmental conditions, including relative humidity. Paajanen et al. 2006 found that for 1.0 and 2.5 μm particles, the adhesion force is constant at low humidities and begins to increase for humidities above 30%. However, for larger particles, the dependency on humidity is not as strong. In their study on the adhesion of 1.0 to 35 μm polystyrene particles, Cleaver and Looi 2007 found that increasing the relative humidity from 2% to 65% had no noticeable impact on adhesion. Polystyrene particles demonstrate hydrophobicity and will not adsorb sufficient water to form a complete meniscus at humidities up to 65%. However, the authors observed a threshold at 65%, in which the particle adhesion increased with applied load. This can be attributed to the plasticizing effect of adsorbed water on the polystyrene, causing plastic deformation at the contact sites between the particle and surface (Note: polystyrene latex particles were used in this research, as discussed in Chapter 3). Coupled with relative humidity is the concept of residence time: the time a particle remains deposited on a surface before resuspension. Ibrahim et al. 2004 demonstrated that exposing a particle to a high humidity environment (61%) for a period of 24 hours considerably reduced particle resuspension due to the significant increase in the total adhesion force. In conclusion, there is sufficient evidence to suggest that the total particle adhesion is a function of relative humidity and that several distinct regions exist: $< 30\%$: minimal impact, > 50 to 65%: significant increase in adhesion, and approaching saturation: rapid decrease in adhesion.

2.1.6 Particle-to-Particle Adhesion

For multilayer deposits, there is a layer of particles that are in contact with the surface, as well as upper layers where particles are in direct contact with other particles. Therefore, unlike in monolayer deposits, adhesion between particles must be considered. Israelechvilli 1994 noted that the interaction energy between two spheres of the same radius is equal to half of the energy between a sphere and a flat surface. Lazaridis and Drossinos 1998 also found that the adhesive potential between a spherical particle and a surface is stronger than that between two spherical particles. The reduced adhesion force associated with particle-to-particle contact suggests that resuspension will likely increase for multilayer deposits compared to monolayer deposits. In addition, for multilayer deposits of polydisperse particles, the relationship between the diameters of the two particles in contact must also be addressed. Zimon 1982 and Friess and Yadigaroglu 2002 examined particle-to-particle interaction and defined the adhesion force between two particles of different sizes as follows:

$$F_{adh,particle-to-particle} = C\left(\frac{\delta_p d_p}{\delta_p + d_p}\right) \tag{10}$$

Where C is a constant of adhesion, δ_p is the diameter of the smaller particle and d_p is the diameter of the adhered particle. As δ_p becomes small relative to d_p, the resulting adhesion force becomes more dependent on the diameter of the smaller particle.

2.2 Particle Resuspension Models

Because resuspension is an important environmental transport mechanism in both the outdoor and indoor environments, it has attracted very strong theoretical and experimental investigations over the past several decades in an attempt to understand the mechanisms that remove stationary particles from surfaces. Resuspension arises from the

competing effects of the aerodynamic removal forces applied by external airflow over a surface and the adhesive forces that act on a deposited particle, as outlined in Section 2.1.

The two aerodynamic forces are lift and drag. For a particle in contact with a surface, the lift force can be calculated as follows (from Leighton and Acrivos 1985, assuming the velocity field in the viscous sublayer as presented in Soltani and Ahmadi 1994, 1995b):

$$F_{lift} = \frac{0.774 \rho u^{*4} d_p^4}{\nu^2} \tag{11}$$

Where ρ is the density of air, u^* is the critical shear velocity, and ν is the kinematic viscosity of air. The drag force can be determined from the following relationship (from O'Neill 1968 and Soltani and Ahmadi 1994, 1995b):

$$F_{drag} = \frac{2.9 \pi \rho u^{*2} d_p^2}{C_C} \tag{12}$$

Where C_C is the Cunningham correction factor, which is a function of the mean free path of air and accounts for "slip" at the particle surface. Lift and drag can be expressed in alternate forms depending on the fluid dynamics over a surface; however, they tend to be proportional to d_p^2 and d_p^4, respectively. As previously discussed, adhesion forces are proportional to d_p. This suggests that as the particle diameter decreases, it becomes increasingly more difficult to resuspend because the adhesion forces become stronger relative to the aerodynamic removal forces.

Sections 2.2.1 through 2.2.4 provide a brief summary of selected monolayer and multilayer resuspension models (a more comprehensive review of resuspension models can be found in Sehmel 1980, Ziskind et al. 1995, and Ziskind 2006). The basis for this classification is as follows: a monolayer model is one in which the model only accounts for particle-to-surface interactions, whereas a multilayer model accounts for particle-to-

particle interactions in a deposit consisting of multiple layers of particles. Furthermore, where possible, the models were broadly classified as either force or energy balances. A force balance models the adhesive and aerodynamic removal forces acting on a particle and an energy balance models the transfer of turbulent energy from the fluid flow to a particle deposited in an adhesive well, and applies JKR theory (Ziskind et al. 1995).

2.2.1 Monolayer: Force Balances

One of the early resuspension models, proposed by Corn and Stein 1965, demonstrated how aerodynamic forces, such as drag and lift, could resuspend a deposited particle from a surface. Their analysis was based on a simplified force balance on a particle in which a particle will resuspend when the drag and lift forces exceed the forces of adhesion. Additional theoretical investigations on the aerodynamic removal of particles have demonstrated the complexity of the phenomenon and the importance of fully characterizing the associated fluid dynamics in ideal and realistic environments. The concept of turbulent bursts penetrating the viscous sublayer (y_{VSL}) of the turbulent boundary layer was first discussed in Cleaver and Yates 1973. Lift forces associated with the common assumption of steady, laminar flow in the viscous sublayer are very small and incapable of resuspending a micron-size particle, however, instantaneous lift forces generated by turbulent bursts may be sufficient (see Illustration 2.2). The authors demonstrated the importance of accurately modeling the flow around a deposited particle since particle resuspension and fluid dynamics are strongly coupled physical phenomena.

Braaten et al. 1990 and Jurcik and Wang 1991 further examined the impact of turbulent bursts on resuspension and proposed that the random, discrete nature of these bursts, both temporally and spatially, may be described by a probability distribution. Their findings that the removal forces are not constant in time agree with those of

Cleaver and Yates 1973 and emphasize the statistical, or stochastic, nature of resuspension. The Reynolds number of the fluid flow can represent the intensity and frequency of the turbulent bursts. Wen and Kasper 1989 found resuspension to increase with increasing Reynolds number, suggesting more frequent penetrations of turbulent bursts into the viscous sublayer will resuspend more particles.

Another fluid dynamics parameter, the acceleration of the flow, can influence particle resuspension. In their development of a generalized transport equation for particles exposed to turbulent flow, Tadmor and Zur 1981 demonstrated how an additional removal force, known as the Basset force, could arise due to the relative acceleration of the fluid flow to the deposited particle. The Basset force will increase the net drag force, thereby reducing the velocity of the bulk airflow required for particle removal from a surface. In addition, the time dependence of resuspension was examined in Hall and Reed 1989, in which resuspension can be divided into two temporal regimes: a short (approximately one second), initial period of high rates of particle detachment, followed by a long period of minimal detachment where resuspension varies inversely with time ($1/t$).

Another perspective on the force balance approach to resuspension was presented by Wen and Kasper 1989, who employed a kinetic particle desorption model, analogous to the desorption of molecules from a surface. In their model, they proposed a non-dimensional adhesion force, defined as the ratio of the adhesion force to the removal force. Following established desorption kinetics theory, they assumed a Langmuir model to relate the surface concentration of particles with a given non-dimensional adhesion force. The authors also accounted for the time dependence of resuspension in their model by introducing terms accounting for the initial resuspension peak of loosely bound particles and the $1/t$ dependence for long, extended periods of resuspension.

A recent force balance model by Ibrahim et al. 2003 discussed the possibility of three modes of particle resuspension: direct lift-off, sliding, and rolling. The resulting resuspension mode depends on the relationship between the lift, drag, and adhesive forces acting on the deposited particle and the static coefficient of friction and contact radius at separation (determined by applying JKR theory). The authors, who also collected experimental data to validate their model, found that rolling is the dominant mode of resuspension and particles do not resuspend through direct lift-off from the surface. Sliding was found to require an unrealistically low static coefficient of friction to occur. The impact of turbulent bursts was also considered in their model and was found to significantly reduce the threshold velocity necessary for resuspension, thereby confirming the early findings of Cleaver and Yates 1973 that turbulent bursts are an important contributing factor to particle removal. A modeling study by Ahmadi et al. 2007 also demonstrated that rolling is the dominant mode of resuspension, in both the presence and absence of a capillary force.

Additional force balance models have investigated the impact of the surface roughness of both the particle and surface. Surface roughness has been found to reduce the adhesion forces acting on a particle and is therefore an important parameter is resuspension models (Greenwood and Williamson 1966). Ahmadi and Guo 2007 proposed a bumpy particle model in which the surface roughness of the particle can be modeled as a number of bumps, representing the asperities. The authors found that higher velocities are necessary to remove particles that have a smaller number of large bumps and that an increase in the spacing between bumps reduces the velocity required for resuspension. Guingo and Minier 2008 also examined the impact of surface roughness on particle resuspension. They proposed two scales of roughness: a fine scale where the roughness is on the order of nanometers and a large scale where the roughness

is on the order of micrometers. They also considered the relationship between particle size and the size of the asperities.

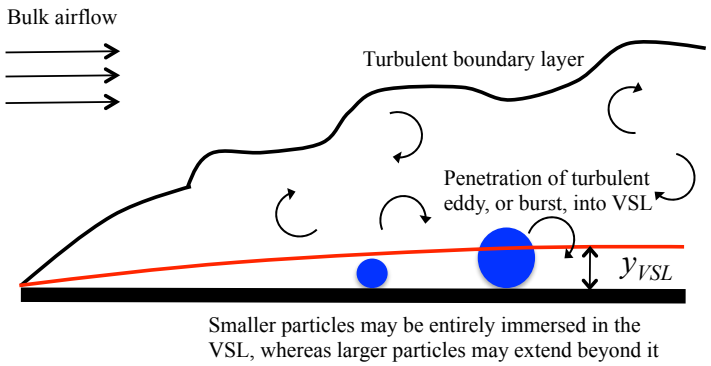

Illustration 2.2: Development of turbulent boundary layer and viscous sublayer (VSL)

2.2.2 Monolayer: Energy Balances

Reeks et al. 1988 presented a new, energy balance approach to modeling resuspension by which a particle will detach once it accumulates sufficient vibrational energy, imparted to it through the turbulent energy of the fluid flow (referred to as the RRH model). The turbulent fluctuations of the flow cause the particle to oscillate in its adhesive potential well. The energy transfer is most efficient when the driving frequencies of the lift force fluctuations near the natural frequency of vibration of the particle. By accounting for resonant energy transfer, the RRH model predicts particle resuspension at lower velocities compared to models based on force balances. Lazaridis et al. 1998 modified the RRH model and calculated the particle adhesion force based on the Lennard-Jones intermolecular interaction potential. They also found that the natural frequency of a particle, which is needed to determine resuspension, depends on its size and composition. Lastly, Reeks and Hall 2001 present the rock'n roll model, which accounts for both drag and lift forces, whereas in the original RRH model, the

aerodynamic removal forces are exclusively lift forces. The rock'n roll model was found to more closely match experimental data produced by the authors, suggesting the importance of accounting for drag forces acting on the particle.

2.2.3 Multilayer

The models discussed thus far in 2.2.1 and 2.2.2 only account for particle-to-surface interactions (monolayer deposit). Several other models have been proposed for multilayer deposits, where particle-to-particle contact becomes an important variable (see Section 2.1.6 for discussion on adhesion). One of the first papers to discuss resuspension from multilayer deposits is that by Fromentin 1989. The author examined the time dependence of multilayer resuspension, finding that the resuspension flux decreases with the time of exposure to a given flow field (follows the trend of Hall and Reed 1989). This is attributed to a decrease in the resuspension of loosely adhered particles with exposure time.

An important distinction between monolayer and multilayer resuspension models is that for monolayer deposits, all deposited particles are assumed to interact with the fluid, whereas in multilayer deposits only the top, or canopy, layer is expected to interact with the fluid (Friess and Yadigaroglu 2001). In their discussion of their multilayer model, Friess and Yadigaroglu 2001 suggest that major discrepancies between theory and experiments are expected if monolayer models are used to represent multilayer deposits of varying thicknesses. Monolayer models will overestimate resuspension for thick, multilayer deposits because they assume all particles interact with the fluid flow. The authors modeled resuspension for a range of finite multilayer thicknesses. Generally, for a given exposure time, their dimensionless resuspension flux increased with increasing thickness, until a saturation effect was observed where additional layers did not impact

resuspension. Lazaridis and Drossinos 1998 also modeled multilayer resuspension and found that the resuspension rate of the surface layer was generally less than that of the canopy layers because the adhesive force between a particle and a surface is greater than that between two particles (as discussed in Section 2.1.6). The authors also found that higher friction velocities are necessary to resuspend surface layer particles compared to particles deposited along the canopy layer.

Matsusaka and Masuda 1996 investigated the resuspension of particle aggregates (or clusters) from a multilayer deposit both theoretically and experimentally. The authors note that the resuspension of aggregates may be more representative of what is actually occurring in industrial aerosol and powder processes. Particles were found to readily resuspend in the form of larger aggregates. This phenomenon has been confirmed by Friess and Yadigaroglu 2002, who modeled the resuspension of particle clusters from multilayer deposits. Particles were found to more easily resuspend in the form of larger clusters than individually because the aerodynamic removal forces are proportional to the square of the diameter whereas adhesion forces between two particles are proportional to the diameter of the smaller particle. In addition, since only small fractions of the particles are in contact with the wall surface, the influence of the surface layer of particles on the overall resuspension can be neglected. The authors also examined the influence of the deposit structure on resuspension and considered two limiting cases: a crusty, cake-like deposit with a low porosity and a fluffy, highly porous deposit with less particle-to-particle contact. The multilayer deposit structure is dependent on the deposition mechanisms, e.g. gravitational settling will likely produce a more fragile, fluffy deposit compared to inertial impaction. The authors found that resuspension increased with increasing porosity, which suggests that fluffy deposits will resuspend more readily than crusty ones. Furthermore, the size of the resuspended clusters was roughly one to four

times greater than the size of the deposited particles and tended to be larger for fluffy deposits compared to crusty ones.

An alternate, energy balance approach to multilayer resuspension was presented in Gac et al. 2008. The authors modeled the interaction between neighboring particles with a harmonic force. They found particles to resuspend in the form of large clusters when both the particle-to-particle adhesive force and the gravitational force were greater than the fluid shear force. Furthermore, particles were found to resuspend individually when the turbulence intensity of the fluid flow is high and can break up deposited particle clusters.

2.2.4 Summary

Section 2.2.1 through 2.2.3 provide a general overview of the various monolayer and multilayer resuspension models. Table 2.1 provides a list of these models and their classification. To date, there are substantially more monolayer models in the literature, and this trend follows for experimental studies. Monolayer models have uncovered a wealth of information on particle resuspension over the past several decades. In summary, these models indicate:

- Resuspension increases with particle size and bulk fluid velocity
- Penetration of turbulent bursts into the viscous sublayer are responsible for increasing resuspension
- Resuspension is strongly dependent on temporal changes in the flow and the total time of exposure
- Rolling is the dominant mode of resuspension
- Variables such as surface roughness, relative humidity, and particle composition influence adhesion, and subsequently resuspension

- Energy balance models tend to be more accurate by accounting for the transfer of energy through turbulent fluctuations
- Multilayer models have shown that the type of deposit, and its structure, can have a significant impact on particle resuspension

Table 2.1: Summary of the deposit modeled in selected resuspension models

Reference	Deposit Modeled	Classification
Corn and Stein 1965	Monolayer	Force Balance
Cleaver and Yates 1973	Monolayer	Force Balance
Tadmor and Zur 1981	Monolayer	Force Balance
Kasper and Wen 1988	Monolayer	Force Balance
Reeks et al. 1988	Monolayer	Energy Balance
Wen and Kasper 1989	Monolayer	Force Balance
Fromentin 1989	Multilayer	Force Balance
Hall and Reed 1989	Monolayer	Force Balance
Braaten et al. 1990	Monolayer	Force Balance
Jurcik and Wang 1991	Monolayer	Force Balance
Matsusaka and Masuda 1996	Multilayer	Force Balance
Lazaridis et al. 1998	Monolayer	Energy Balance
Lazaridis and Drossinos 1998	Multilayer	Force Balance
Friess and Yadigaroglu 2001	Multilayer	Force Balance
Reeks and Hall 2001	Monolayer	Energy Balance
Friess and Yadigaroglu 2002	Multilayer	Force Balance
Ibrahim et al. 2003	Monolayer	Force Balance
Ahmadi and Guo 2007	Monolayer	Force Balance
Ahmadi et al. 2007	Monolayer	Force Balance
Guingo and Minier et al. 2008	Monolayer	Force Balance
Gac et al. 2008	Multilayer	Energy Balance

2.3 WIND TUNNEL STUDIES

The diversity apparent in the myriad of resuspension models proposed over the past several decades is also exhibited in the various experimental investigations on resuspension. The most common method to study aerodynamic resuspension is to place a seeded sample in a wind tunnel test chamber and expose it to various airflow conditions, e.g. velocity, turbulence, and acceleration. This method provides a systematic means to evaluate the impact of the multitude of variables that influence particle adhesion and resuspension. This section will provide a summary of selected wind tunnel studies, broadly classified as either monolayer or multilayer, and the relevant findings of each.

Generally, particle resuspension is often expressed as either a resuspension rate or an absolute resuspension fraction (also referred to as percent removal, detachment fraction, fraction of resuspension, entrainment efficiency, or resuspension efficiency in the literature) (Nicholson 1988). The resuspension rate, Λ in s^{-1}, is defined as follows:

$$\Lambda = \frac{resuspension\ flux[g\,m^{-2}\,s^{-1}]}{initial\ surface\ concentration[g\,m^{-2}]} \tag{13}$$

The absolute resuspension fraction, Φ in (- or %), is defined as:

$$\Phi = \frac{\#\ of\ particles\ resuspended\ during\ test\ flow\ conditions[\#\,p\,m^{-2}]}{initial\ surface\ concentration\ [\#\,p\,m^{-2}]} \tag{14}$$

The initial surface concentration is also referred to as the seeding density and is expressed as the number of particles (p) per unit area. The resuspension rate is often plotted against time, whereas the absolute resuspension fraction is reported for a given exposure time. The metric presented in this study is an absolute resuspension fraction (Section 3.1). A list of empirical models for the two metrics is presented in Kim et al. 2010. To experimentally determine the two metrics, two methods are typically employed: sampling of the airborne particle concentration at the outlet of the wind tunnel or particle counting via optical or fluorescence microscopy methods, the later of which

was applied in this study. Lastly, another resuspension metric has been proposed by Mukai et al. 2009, the relative resuspension fraction, Γ (- or %), defined as follows:

$$\Gamma = \frac{resuspension\,at\,test\,conditions[\#\,p\,m^{-3}]}{\max imum\,possible\,resuspension[\#\,p\,m^{-3}]} \tag{15}$$

As with the absolute resuspension fraction, the relative resuspension fraction is reported for a given exposure time. The relative resuspension fraction avoids particle counting or determining the initial surface concentration of particles. The total achieved resuspension is the sum of the resuspension that occurs during the test flow conditions and the maximum resuspension when the seeded sample is exposed to high velocity impinging jets.

Predominately, wind tunnel studies have focused on resuspension from monolayer deposits, where there is minimal to no particle-to-particle contact. Particle counting methods typically require that particles be sparsely deposited on a sample so they can be easily distinguished from one another. Furthermore, as demonstrated in Section 2.2, the majority of resuspension models are based upon monolayer deposits. Experimental studies have likely followed this trend in part to validate theoretical models. Only a few papers have examined multilayer resuspension experimentally, e.g. Fromentin 1989 and Matsusaka and Masuda 1996. Friess and Yadigaroglu 2001 (Section 2.2.3) note the need for more experiments on the resuspension of multilayer deposits of varying thicknesses. The following two sections will provide an overview of relevant monolayer and multilayer wind tunnel studies.

2.3.1 Monolayer

Monolayer resuspension experiments have demonstrated that a number of variables can influence resuspension, notably: particle size, air velocity, surface material and roughness, particle composition, characteristics of the fluid flow, relative humidity,

and residence time. The term threshold velocity will be used in the following discussion, which is the velocity at which 50% of the particles resuspend for a given set of conditions.

2.3.1.1 Particle Size and Velocity

One of the first wind tunnel resuspension studies was that by Corn and Stein 1965. A critical finding of their research was the particle size dependence of resuspension: resuspension will increase with increasing particle size. Smaller particles are more likely to be completely immersed the viscous sublayer where they will not experience the enhanced removal associated with turbulent eddies. This thickness of this layer, y_{VSL}, can be reduced by increasing the bulk air velocity, which subsequently increases the resuspension for a given particle size (y_{VSL} is proportional to the inverse of the bulk air velocity, Bejan 2004).

The findings of Corn and Stein 1965 have since been confirmed in many wind tunnel studies. For example, Ibrahim et al. 2003 found the threshold velocity for glass microspheres to increase from 5 m/s for 72 μm to 16 m/s for 32 μm. Nicholson 1993 found resuspension rates to increase with increasing particle diameter from 4.1 to 22.1 μm. Depending on surface roughness, Jiang et al. 2008 observed threshold velocities of 70 to 80 m/s for 41 μm glass beads and 95 to 175 m/s for 22 μm glass beads.

Another important finding relevant to particle resuspension in the indoor environment is the resuspension of particles in the inhalable coarse size range, 2.5 to 10 μm, from monolayer deposits. Several studies have suggested that very high velocities, unrealistic of what would occur indoors, are necessary to induce resuspension of particles within and near this size range from monolayer deposits. Corn and Stein 1965 discovered that an air velocity of 117 m/s would only resuspend 32% of 10.6 μm glass

beads. Similarly, Jiang et al. 2008 determined threshold velocities as high as 100 to 165 m/s for 11 μm PMMA particles. Another related study by Ziskind et al. 2002 on the resuspension of particles by pulsed air jets found that jet velocities of 100 to 200 m/s were required to resuspend 2 to 5 μm particles, with resuspension fractions ranging from roughly 0.20 to 0.90. Although larger particles (~20 to 110 μm) will resuspend at lower velocities, as demonstrated in Ibrahim et al. 2003 and 2008, these particles are generally not of concern from an indoor environmental quality perspective. They will likely remain airborne for very short periods due to their high settling velocities and are also efficiently removed in the upper respiratory system and therefore do not pose a serious health risk (Hinds 1999).

2.3.1.2 Surface Material and Roughness

The characteristics of the sample surface the particles are in contact with also influence resuspension. The Hamaker constant between a particle and a surface and the hydrophobicity of a surface will affect the adhesive forces acting on a particle (Section 2.1). Many monolayer resuspension experiments have been conducted using glass (e.g. Braaten 1994, Ibrahim et al. 2003, 2004, 2008) samples and there are limited studies that have systematically investigated resuspension from different surfaces. Wu et al. 1992 found that resuspension of lycopodium spores (30 μm in diameter) was significantly greater for glass compared to plexiglass due to the enhanced electrostatic adhesion of the plexiglass. Mukai et al. 2009 investigated resuspension of potassium chloride particles (1 to 20 μm) from three indoor surfaces: galvanized sheet metal, linoleum, and carpet. Carpet exhibited the greatest resuspension, followed by linoleum, and then by galvanized sheet metal.

Carpet is a very complex surface and particles deposited along the canopy of the fibers are likely exposed to greater velocities than those deposited on flat surfaces (Mukai et al. 2009). Nicholson 1993, who investigated resuspension from grass and concrete, noted that because grass is fibrous and non-rigid, the grass blades will likely oscillate in the wind, inducing higher levels of turbulence and increased momentum transfer to deposited particles along the blade. However, some particles might become embedded deep into the blades with time, where they will be less likely to resuspend. This same phenomenon may be occurring within the individual fibers of carpet and could lead to greater resuspension short times after deposition and reduced resuspension for extended periods as particles migrate to positions deeper within the fibers.

Particle resuspension is also influenced by surface roughness (Section 2.2.1). Jiang et al. 2008 investigated resuspension from stainless steel of varying average surface roughness, 0.01 μm to 1.64 μm. The authors found the threshold velocity to decrease with increasing submicron-scale surface roughness (from 0.01 to 0.3 μm) due to a reduction in the contact area between the particle and the surface. However, for micron-scale surface roughness (0.3 to 1.64 μm), the threshold velocity was not strongly dependent on roughness because micron-scale roughness does not effectively reduce the adhesion force.

2.3.1.3 Particle Composition

The impact of the particle composition has also been explored in wind tunnel resuspension studies. Wu et al. 1992 explored resuspension of uranine particles, polystyrene/divinylbenzene particles, lycopodium spores, and two types of pollen. Low resuspension was found for uranine and polystyrene/divinylbenzene particles, although actual data was not provided. The wind tunnel experiments were performed at relative

humidities in the range of 58 to 78%, and as discussed in Section 2.1.5, polystyrene may plastically deform at relative humidities above 65%, resulting in enhanced adhesion and reduced resuspension. Lycopodium spores were found to resuspend in significant fractions at very low velocities (4 to 8 m/s). Ibrahim et al. 2003 reported a similar trend, with threshold velocities for 30 μm lycopodium spores roughly half of those as found for 32 μm glass microspheres. Lycopodium spores are spheres with small bars along it surface, which significantly reduce its contact area and therefore the adhesion force with the sample surface (Nitschke and Schmidt 2009). Braaten 1994 also found the threshold velocity of 28 μm lycopodium spores (8.73 m/s) to be slightly less than that for 34 μm timothy pollen (12.57 m/s) and 30 μm glass microballoons (9.72 m/s).

Ibrahim et al. 2003 also compared resuspension of glass and stainless steel microspheres under the same test conditions. 70 μm stainless steel microspheres had a lower threshold velocity, 3 to 4 m/s, compared to that of the 72 μm glass microspheres, 5 to 6 m/s. The authors attributed this to the reduced adhesion of stainless steel microspheres on glass samples relative to the glass microspheres on glass samples.

2.3.1.4 Flow Characteristics: Exposure Time, Acceleration, and Turbulence

The time a seeded sample is exposed to the flow conditions in a wind tunnel will impact particle resuspension. Wu et al. 1992 confirmed the findings of Hall and Reed 1989 and found that two distinct temporal regimes existed: a short period of less than one minute with very high resuspension, and an extended period of minimal resuspension. Nicholson 1993 investigated resuspension for exposure times of 10 to 3600 seconds, and found that almost half of the resuspended particles were removed in the first 10 seconds. The resuspension rate generally decreased by three orders of magnitude over 3600 seconds of exposure.

The acceleration of the flow during the initial period of exposure is likely responsible for the enhanced resuspension. Ibrahim et al. 2003 also found that two distinct temporal regimes exist, a period of high resuspension during the acceleration of the flow up to the steady-state velocity, and a period of low resuspension during steady-state flow. As discussed in Tadmor and Zur 1981, an additional aerodynamic removal force, known as the Basset force, can arise as the flow is accelerated. Ibrahim et al. 2003 found that the resuspension rate during the acceleration period (4.6 s^{-1}) is roughly six hundred times greater than during the steady-state period (0.0075 s^{-1}). The authors also suggest that the duration of the acceleration period is important. To achieve higher resuspension for lower steady-state velocities, longer periods of acceleration are required. Ibrahim and Dunn 2006 examined the impact of acceleration on the threshold velocity of stainless steel microspheres and found the threshold velocity to increase with increasing acceleration in the range of 0.3 to 2.0 m/s^2. The reduction in the resuspension fraction for higher accelerations is due to the shorter period of acceleration before steady-state conditions are obtained.

Ibrahim et al. 2004 also studied the impact of turbulence. The threshold velocity for turbulent flow (Reynolds number of 1.05 x 10^6) was 8.2 m/s, whereas for laminar flow (Reynolds number of 1.05 x 10^5) it was 17.7 m/s. Mukai et al. 2009 observed a similar phenomenon and found threshold velocities (based upon the relative resuspension metric) to decrease with increasing turbulence intensity of the fluid flow. The penetration of turbulent bursts into the viscous sublayer (Cleaver and Yates 1973) and transfer of turbulent energy to a deposited particle (Reeks et al. 1988) are likely responsible for enhanced particle resuspension. Therefore, by increasing the turbulence of the fluid flow, which can be accomplished without necessarily increasing the bulk air velocity (Mukai et al. 2009), the frequency at which turbulent bursts penetrate will likely increase, as well as

the turbulent energy imparted to the particle through fluctuations in the flow. As discussed in Mukai et al. 2009, turbulent flow is often associated with flow across joints in ventilation systems and air currents generated by walking, and is therefore an important variable in particle resuspension.

2.3.1.5 Relative Humidity and Residence Time

Ibrahim et al. 2004 is one of the few studies to systematically investigate the combined impact of relative humidity and residence time on resuspension. As previously discussed in Section 2.1.5, the total adhesion force acting on a particle is dependent on the relative humidity of the surrounding air. As demonstrated in Ibrahim et al. 2004, increasing both the relative humidity and the residence time in which a particle sits on a surface increased the threshold velocity. For example, at 30% relative humidity and a very short residence time, the threshold velocity for stainless steel microspheres (64 to 76 μm) was 4.2 m/s. For the same residence time, but at 61% relative humidity, the threshold velocity increased to 10.7 m/s. By increasing the residence time to 24 hours, the threshold velocities increased to 5.5 m/s and much greater than 24 m/s (actual value not reported) for 30% and 61% relative humidities, respectively. This suggests that the impact of moisture in the ambient air on the total adhesion force is a time-dependent process. Some wind tunnel studies exposed seeded samples to the test flow conditions a short time after the particles were deposited (residence of several minutes to hours) (e.g. Nicholson 1993, Ibrahim et al. 2003). Based on the findings of Ibrahim et al. 2004, it is likely that the resuspension rates and fractions presented in these studies would decrease for longer residence times.

2.3.1.6 Seeding Density

Another factor that has been found to influence resuspension is the seeding density (surface concentration) of particles on a sample surface. Ibrahim et al. 2004 found that by increasing the seeding density from 0.5 particles/mm^2 to 3 particles/mm^2, the threshold velocity decreased from 4.2 m/s to 2.5 m/s. Greater seeding densities tend to result in a higher probability of particle collisions as particles roll along the surface and begin to detach. Collisions between deposited particles can induce resuspension by applying an additional removal force that could help overcome the total adhesion force. The impulsive force generated by the collision is linked to the mass of the particles involved. Ibrahim et al. 2004 used stainless steel microspheres with a density of 8000 kg/m^3, which likely enhanced the impact of collisions on resuspension relative to a less dense material such as polystyrene (1000 kg/m^3).

2.3.1.7 Summary

The preceding discussion provided an overview of the major discoveries of monolayer wind tunnel resuspension studies. Collectively, these papers have demonstrated that eleven variables can influence particle resuspension: air velocity, particle diameter, surface material, surface roughness, particle composition, wind tunnel exposure time, flow acceleration, turbulence intensity/Reynolds number, relative humidity, residence time, and seeding density. It would be difficult to systematically study each of these variables experimentally within the scope of a single research project, however, the preceding review of the existing literature provides a strong basis from which to build upon in future research.

Figure 2.2 provides a summary of monolayer wind tunnel studies that have reported threshold velocities, or provided data from which threshold velocities could be estimated. As per the discussion in 2.3.1.1, very high velocities are generally required for

small particles, especially those in the inhalable coarse size range. Additional information for selected wind tunnel experiments can be found in Table 2.2.

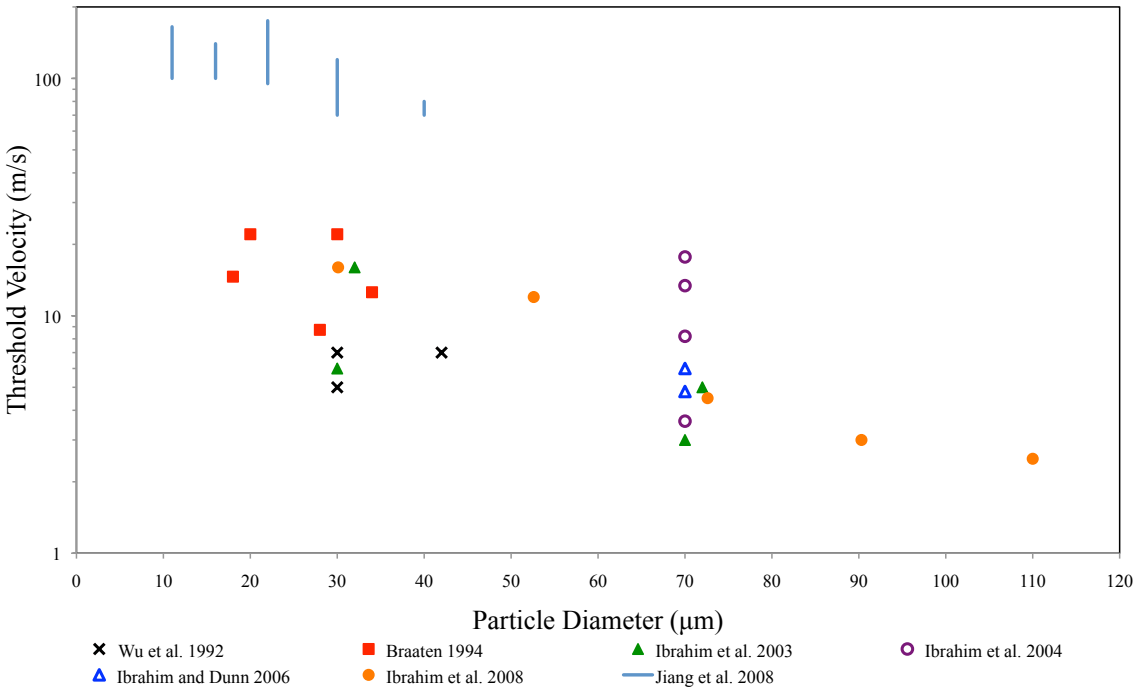

Figure 2.2: Threshold velocities from selected monolayer wind tunnel resuspension studies

2.3.2 Multilayer

Multilayer resuspension has received considerably less attention in the literature, and only a few wind tunnel studies have studied this type of deposit. In their wind tunnel study on the emissions of road dust, Chiou and Tsai 2001 noted that models based on monolayer deposits cannot be applied to resuspension in field conditions where multilayer deposits of polydisperse particles exist. In addition, Matsusaka and Masuda 1996 remarked that multilayer deposits might be more representative of realistic deposits in industrial aerosol and powder processes. Furthermore, it is likely some variation of multilayer deposits can be found in the indoor environment as particles accumulate on the

floor or surfaces of ventilation ducts. To date, there are no systematic experimental evaluations of the impact of multilayer deposit characteristics, such as thickness, porosity, and structure, on resuspension.

Fromentin 1989 investigated the time dependence of resuspension from multilayer deposits, finding that resuspension decreases with time, which follows the trend for monolayer deposits. Chiou and Tsai 2001 reported a similar trend, finding that the loosely bound particles along the uppermost layers would resuspend initially, leaving behind strongly bound particles on the surface (corroborating the model predictions of Lazaridis and Drossinos 1998). The authors also found the resuspension flux of road dust (in kg/m^2-s) to increase with the rate of acceleration of the flow.

Matsusaka and Masuda 1996 studied the resuspension of particle clusters from multilayer deposits. They deposited a multilayer of 3 μm fly ash particles and found small clusters, with diameters ranging from 10 to 30 μm, to resuspend is a random manner. This confirms the work of Friess and Yadigaroglu 2002, who modeled the resuspension of particle clusters and found the resuspended clusters to be larger than the deposited particles. With time, the resuspension process progressed through the depth of the multilayer deposit, and the uppermost layer was continually renewed. Resuspension was found to increase with both air velocity and acceleration, and was detected at velocities between 10 and 40 m/s. In addition, following the trend of Ibrahim et al. 2003, resuspension was greater during the period of transient flow compared to steady-state flow. Lastly, Gac et al. 2008 discovered that as particle clusters resuspend from a multilayer deposit and become airborne, they may break apart due to aerodynamic forces generated by turbulent flow.

2.3.3 Summary

Sections 2.3.1 and 2.3.2 provided a summary of wind tunnel experiments on monolayer and multilayer particle resuspension. A summary of the experimental parameters in each study is provided in Table 2.2. It is evident that substantially more empirical data exists for monolayer deposits compared to multilayer deposits. Monolayer studies have provided valuable insight on the variables that can influence resuspension and have often validated numerous models. Two important distinctions between the two types of deposits are presented below:

- Resuspension of inhalable coarse particles occurs at much lower air velocities for multilayer deposits. Chiou and Tsai 2001 and Matsusaka and Masuda 1996 found significant resuspension to occur at velocities between 10 and 40 m/s. Based on the findings of Corn and Stein 1965 and Jiang 2008, velocities near and above 100 m/s are necessary to induce resuspension of particles near this size range from monolayer deposits. These results confirm the model of Lazaridis and Drossinos 1998, which demonstrated that the upper layers of multilayer deposits resuspend at lower velocities compared to the surface layer.
- In multilayer deposits, particles will likely resuspend in the form of larger clusters, which may break apart once airborne.

Table 2.2: Summary of experimental parameters for wind tunnel resuspension studies

Reference	Deposit	Surface Loading Mono: Seeding density Multi: Particle loading	Surface(s)	Particle Type(s) & Size Range	Environmental Conditions	Velocity Range	Additional Variables Studied
Wu et al. 1992	Monolayer	50 to 100 particles per microscope image	Glass, plexiglass, white oak leaves	Uranine, polystyrene/divinylbenzne, lycopodium spores, paper mulberry pollen, Johnson grass pollen: 5 to 42 µm (mono)	RH: 58 to 78%	<2 to 8 m/s	Exposure time Turbulence
Nicholson 1993	Monolayer	Not reported	Concrete, grass	Silica spheres: 4 to 22 µm (mono)	Not reported	3 to 8 m/s	Exposure time
Braaten 1994	Monolayer	~5 p/mm^2	Glass	Lycopodium spores, timothy pollen, glass microballoons, glass spheres, nickel spheres: 18 to 34 µm (mono)	RH: 65 to 70% and winter conditions	3 to 20 m/s	None
Ibrahim et al. 2003	Monolayer	~1 p/mm^2	Glass	Stainless steel: 70 µm (mono) Glass: 32 & 72 µm (mono) Lycopodium spores: 30 µm (mono) Stainless steel: 10 to 65 µm (poly)	RH: 25±3%	0 to 25 m/s	Exposure time Acceleration
Ibrahim et al. 2004	Monolayer	~0.5 to 3 p/mm^2	Glass	Stainless steel: 70 µm (mono)	RH: 18 to 67%	0 to 24 m/s	Turbulence Relative humidity Residence time Seeding density
Miguel et al. 2005	Monolayer	Not reported	Flooring material	Fluorescent latex: 0.7 to 4 µm (mono)	RH: 54 to 96%	0.025 to 0.05 m/s	None
Ibrahim and Dunn 2006	Monolayer	~50 p/mm^2	Glass	Stainless steel: 70 µm (mono)	RH: 30±3%	0 to 12 m/s	Acceleration
Jiang et al. 2008	Monolayer	Not reported	Stainless steel (varying roughness)	Glass beads: 20 to 40 µm (mono) PMMA: 11 to 41 (mono)	RH: 35 to 50%	0 to 300 m/s	Surface roughness
Ibrahim et al. 2008	Monolayer	~50 p/mm^2	Glass	Glass: 30 to 110 µm (mono)	RH: 29±3%	0 to 25 m/s	None
Ibrahim et al. 2009	Monolayer	~50 p/mm^2	Clean & dusty glass	Stainless steel: 70 µm (mono)	RH: 19±3%	0 to 18 m/s	Dusty surface
Mukai et al. 2009	Monolayer	Not reported	Linoleum, galvanized sheet metal, carpet	Potassium Chloride (KCl): 1 to 20 µm (poly)	RH: 61 to 69%	5 to 25 m/s	Turbulence
Fromentin 1989	Multilayer	100 to 1000 g/m^2	Not reported	Fe_2O_3, Si, Sn + Fe_2O_3 + NaCl: 2 µm	Not reported	5 to 20 m/s	Exposure time
Matsusaka and Masuda 1996	Multilayer	Not reported	Not reported	Fly ash 3 µm (mono)	RH: 16 to 38%	0 to 40 m/s	Exposure time Acceleration Packing fraction
Chiou and Tsai 2001	Multilayer	Not reported	Aluminum cell	Road dust 0 to 29.1 µm	RH: 55 to 75%	0 to 15 m/s	Exposure time Acceleration Edge effect
Gomes et al. 2007	Multilayer	0.5, 2.5, 6.2 g/m^2	Linoleum, carpet, plastic grass	German roach allergen: 2.1 to > 9 µm Quartz dust: 0.3 to 16 µm Dust mite: 0.2 to > 2 µm Spores: 0.3 to > 2 µm	RH: 40 to 70%	0.4 to 1.5 m/s	Exposure time Relative humidity Vibration Dust load

Chapter 3: Experimental Methodology

An experimental methodology was developed to determine particle resuspension from monolayer and multilayer deposits. The details of the method are discussed in the following sections. To represent the range of particles in the inhalable coarse size range, two particle diameters were studied: 3 and 10 μm. Two indoor materials were also selected: linoleum, manufactured from linseed oil and wood flour, to represent a common flooring material, and galvanized sheet metal, which is typically used to manufacture ventilation ducts. Because relative humidities may fluctuate from one climate and/or season to another, resuspension experiments were conducted at two relative humidities, 35% and 70%. The samples were seeded with tracer particles and then exposed to various flow conditions in a micro-scale wind tunnel. A fluorescence stereomicroscope was employed to detect the deposited particles on the sample surface and a morphometry program was developed to count the number of particles.

3.1 Absolute Resuspension Fraction

As discussed in Section 2.3, the resuspension metric used in this study is an absolute resuspension fraction, Φ. The absolute resuspension fraction is defined as the change in seeding density before and after the seeded sample is exposed to a given flow condition in the wind tunnel, divided by the initial seeding density. It varies between 0, in which there is no detectable resuspension, and 1, for maximum resuspension.

$$\Phi = \frac{\sigma_i - \sigma_f}{\sigma_i} \tag{16}$$

The initial, σ_i, and final, σ_f, seeding densities are expressed in the number of particles per unit area, #p/mm^2. The absolute resuspension fractions presented in this study are reported for a 100 second wind tunnel exposure time.

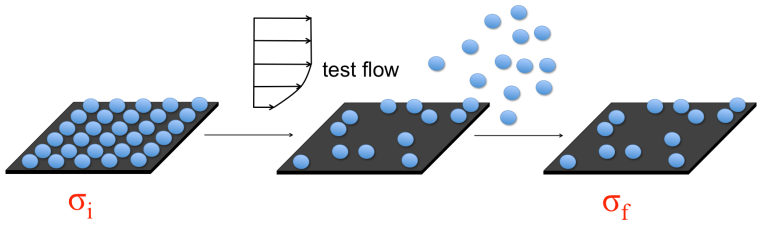

Illustration 3.1: Visual representation of the absolute resuspension fraction

3.2 Particle Seeding

To generate the monolayer and multilayer deposits, two seeding methods were employed. An aqueous solution of internally dyed spherical fluorescent particles (Thermo Scientific) was used to generate a sparse monolayer deposit. To easily distinguish between particle sizes and to forgo actual measurement of individual particles, a specific fluorescent dye was used to represent a particle diameter: red dye for 3 μm and green dye for 10 μm. The fluorophores incorporated into the particle absorb light at one wavelength (excitation) and then emit light at a lower frequency (emission wavelength) (see Table 3.1). The actual size of the supplied particles was verified via air sampling with an aerodynamic particle sizer (APS).

To generate the fluorescent particles for the monolayer deposit, the highly-concentrated aqueous solution was first diluted with commercially available, 99% isopropyl alcohol; a volatile chemical that easily evaporates, permitting the particles to dry quickly, and does not degrade the particles. The diluted solution was then placed in a three-jet Collison Nebulizer (BGI, Inc.). Filtered, pressurized air supplied by the laboratory's compressed air system is directed into the Collison Nebulizer at 137 kPa, where it disperses between three jets into the diluted solution. Isopropyl alcohol droplets are subsequently generated, carrying the fluorescent particles with the effluent air stream. Because a residual electrostatic charge can accumulate on the particles with the glass jar of the nebulizer, the particle stream was passed through a TSI Kr-85 Aerosol Charge

Neutralizer to ensure all particles have a Boltzmann charge distribution. As discussed in Section 2.1.2, electrostatic charge can enhance the adhesion between a particle and a surface. The charge neutralizer helps provide a more uniform adhesive force distribution among the deposited particles and prevents any outlying particles from experiencing increased electrostatic adhesive forces.

The neutralized particle stream is then directed into the seeding chamber, as shown in Figure 3.1. The seeding chamber for the monolayer fluorescent particles has a volume of 50 L and is internally lined with grounded aluminum tape to minimize particle loss to deposition on the sidewalls. A small DC voltage fan ensures the chamber particle concentration remains uniform, which was subsequently verified by assessing the seeding density uniformity amongst the samples (seeding density coefficient of variance amongst samples was generally below 5%, Appendices A.1 and A.2). The samples were placed at the bottom of the chamber on a grounded tray. Each sample was 4.5 by 4.5 cm in size and thoroughly cleaned with 99% isopropyl alcohol to minimize surface contamination and residual electrostatic charges. A steady-state particle concentration was reached after an injection period of 15 minutes (the nebulizer discharge produces an air exchange rate of approximately 6 h^{-1}), after which the particles were deposited via gravitational settling for approximately 6 hours. The seeded samples were then placed in a conditioning chamber for 24 hours prior to wind tunnel exposure, where the relative humidity was controlled and recorded with a HOBO data logger. Two relative humidities were investigated: 35 and 70%. As demonstrated in Ibrahim et al. 2004, the coupled effects of relative humidity and residence time can significantly influence particle resuspension. The humidities were selected to represent both a dry and moist indoor environment. The residence time of 24 hours was chosen to realistically represent the time in which

deposited particles remain on surfaces indoors, which is likely on the order of hours or days, and to allow the meniscus to fully develop for both humidities.

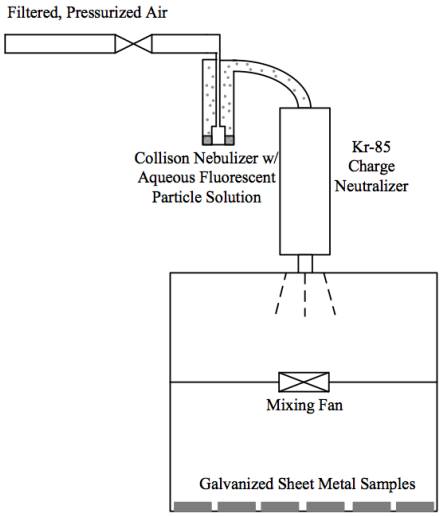

Figure 3.1: Particle seeding chamber for fluorescent particles (0.35 x 0.35 x 0.4 m)

To generate the multilayer deposit, two seeding chambers and three seeding stages were required. Firstly, a surface layer of 10 μm fluorescent particles was deposited in a sparse monolayer employing the aforementioned seeding method. The purpose of the surface layer was to ascertain how the first layer of particles behaves when particle-to-particle contact existed with the upper layers. The seeded samples were then placed in a second seeding chamber (Figure 3.2), where they were seeded with a multilayer deposit of polydisperse (1 to 20 μm) ISO 12103-1 A1 Ultrafine Arizona test dust (ATD). ATD was chosen over latex and silica microspheres and potassium chloride particles because it is both inexpensive and easily generated in large quantities. An improvised aerosolizing chamber was developed in which roughly 20 g of ATD was contained and an impinging jet of filtered air aerosolized the powder, which was then evenly dispersed through small inlets of the aerosolizing chamber into the well-mixed seeding chamber. The ATD loading was measured using gravimetric methods and found

to be approximately 28 g/m^2, similar to that studied in the indoor chamber experiments by Qian and Ferro 2008 (20 g/m^2), but less than that studied in the multilayer wind tunnel experiments of Fromentin 1989 (100 to 1000 g/m^2). The heavy dust load and the visible thickness of the deposit ensured the existence of a multilayer deposit, although the number of layers was not determined. Lastly, the samples were then seeded with a monolayer of 3 μm particles on the canopy of the existing multilayer deposit. The canopy layer was used to assess the impact of the multilayer deposit and particle-to-particle contact on the absolute resuspension fraction when compared to the monolayer experiments. The surface and canopy layers were distinguished by the different fluorescent dyes used for the 3 and 10 μm particles. It is important to note that the absolute resuspension fractions are only reported for these two layers and do not represent the fraction of particles removed from the entire ATD deposit. Future research efforts will be aimed at determining a resuspension metric representative of the entire deposit, but the canopy and surface layers have provided valuable insight into the impact of the deposit on resuspension thus far.

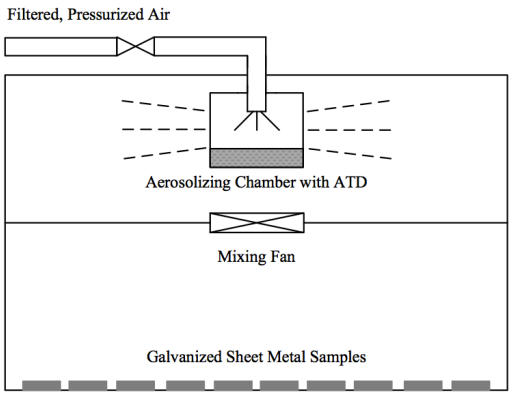

Figure 3.2: Particle seeding chamber for ATD (0.41 x 0.41 x 0.45 m)

3.3 MATERIAL CHARACTERIZATION

As discussed in Section 2.2.1 and 2.3.1.2, the surface roughness of the sample material can impact resuspension. To provide some additional insight on whether the surface roughness is significantly different between linoleum and galvanized sheet, the surface characteristics of the samples were analyzed using a Dektak 6M stylus profilometer. (access to the profilometer was provided by the Nano Fabrication and Characterization Facility at The University of Texas at Austin). Six to ten 2 cm scans were collected for both linoleum and galvanized sheet metal. Glass microscope slides were also analyzed to provide a benchmark for the other two materials. A total of 42,000 data points were collected over the scan distance.

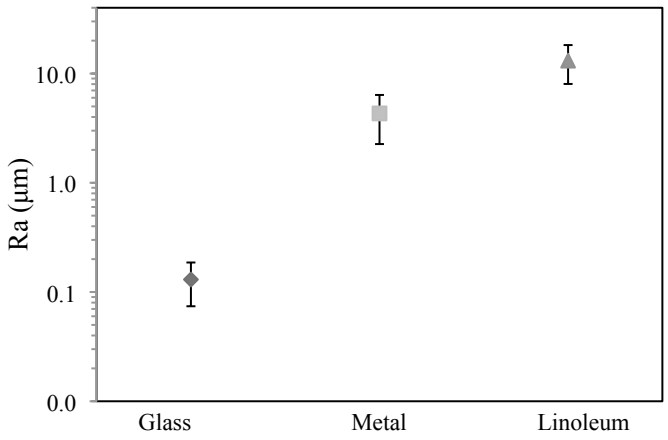

Figure 3.6: Average surface roughness, *Ra*, values for glass, galvanized sheet metal, and linoleum

Both roughness and waviness parameters were calculated for each material. The average roughness, *Ra*, (same parameter as that reported in Jiang et al. 2008) is defined as the arithmetic average deviation from the mean line. The average surface roughness for each of the three materials is reported in Figure 3.6. Linoleum and galvanized sheet metal have similar roughness, 13.13 and 4.31 μm, respectively. They are an order

magnitude greater than polished glass, 0.13 μm. These values are comparable to those found for vinyl flooring in El Hamdani et al. 2008 (1.52 to 5.91 μm) and for stainless steel in Jiang et al. 2008 (micron-scale: 0.3 to 1.64 μm). It should be noted that this is a micron-scale roughness, as in Jiang et al. 2008. A nano-scale roughness also exists, which would more likely influence the effective contact area between a particle and a surface, however, this was not examined in this study.

In addition to determining the average roughness for each material, surface roughness profiles were also generated. Examples for galvanized sheet metal are provided in Figures 3.4 and 3.5, for two scan lengths: 700 and 100 μm, respectively (please note that different scales are used for the x and y axes). Figure 3.4 shows that the profile has an average roughness of several microns over the extended scan length, however, zooming into a shorter region of 100 μm (denoted by red arrow), we see that the profile becomes fairly flat relative to the size of the 3 and 10 μm particles. This suggests that in near vicinity of the particle, the surface appears flat, however, the overall roughness of several microns may give rise to turbulent eddies in the viscous sublayer. Roughness profiles for linoleum exhibited similar trends, although it had a more wavy profile compared to the galvanized sheet metal.

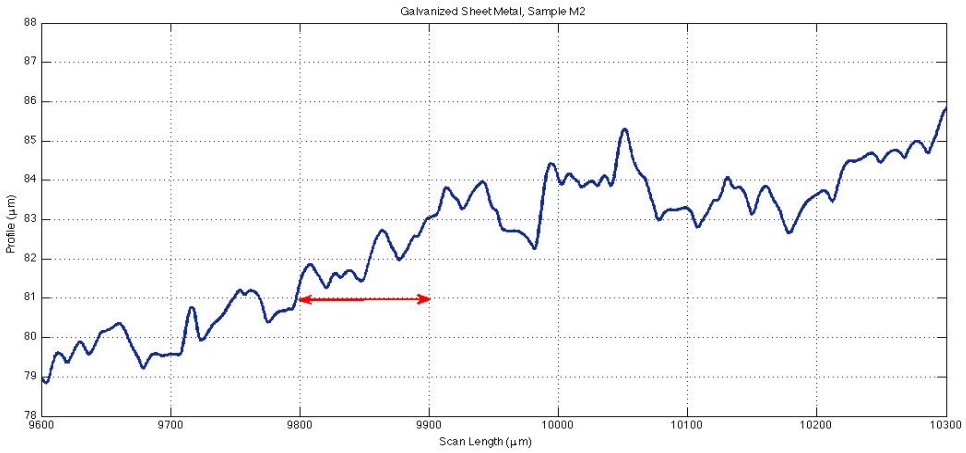

Figure 3.4: Galvanized sheet metal surface roughness profile, 700 µm

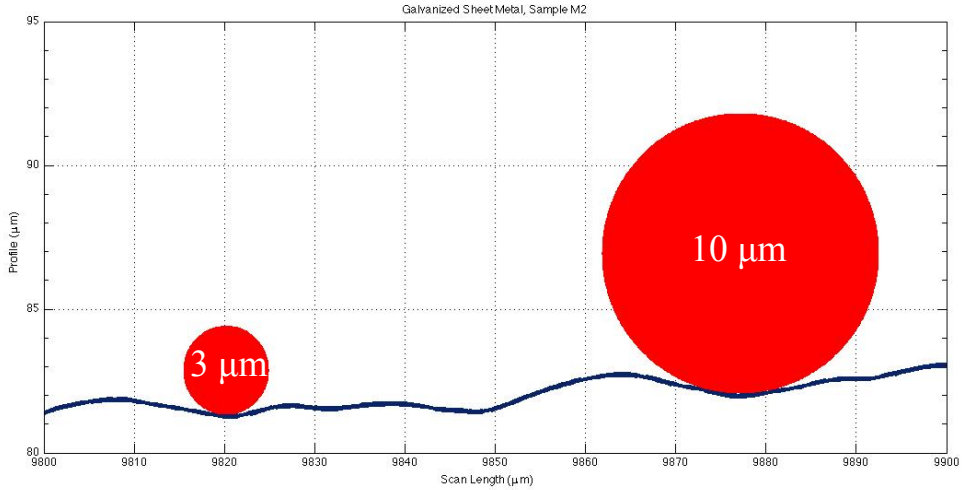

Figure 3.5: Galvanized sheet metal surface roughness profile, 100 µm

3.4 Design of Micro-Scale Wind Tunnels

To study aerodynamic induced particle resuspension from monolayer and multilayer particle deposits, two micro-scale wind tunnels were designed and built. For the monolayer deposits, it was expected that very high velocities would be required to resuspend particles (based on the findings of Corn and Stein 1965 and Jiang et al. 2008).

To achieve air velocities of 25 to 100 m/s, a turbulent wall jet was used. For the multilayer deposits, resuspension occurred at much lower air velocities (< 25 m/s), so a rectangular duct design was used. Filtered, compressed air was supplied to the wind tunnels and regulated via a needle valve positioned upstream of the wind tunnel. The rate at which the valve opened was controlled by a high torque electric motor operating at a constant voltage of 6 V. The valve opening speed regulated the acceleration of the flow and prevented a large spike in the velocity at the commencement of a wind tunnel experiment. As demonstrated in Ibrahim et al. 2003, the acceleration of the flow can influence particle resuspension, so it was desired to maintain relatively constant acceleration rates for all the velocities studied.

The high velocity wind tunnel used for the monolayer deposits has a rectangular cross section that is 5 cm wide by 1.25 cm tall to accommodate the small samples used in this research and is 20 cm in length. The wind tunnel was built using custom laser cut 0.25 inch acrylic sheets and assembled with an acrylic adhesive to ensure an air tight assembly. The wall jet was created via a 1 mm by 5 cm rectangular nozzle positioned immediately upstream of the sample, as shown in Figure 3.6. Due to the high pressure drop across the nozzle (up to 5 psi), the jet exhibited a very uniform discharge. The wind tunnel used for the multilayer deposits was 5 cm wide by 1.25 cm tall and 35 cm long. A flow straightener with 92, 1.5 mm circular holes was positioned 22 cm upstream of the sample to help dissipate the air jets created by the two inlets and to improve flow uniformity.

Computational fluid dynamics was used in the design phase for both wind tunnels. The wind tunnels were modeled in the CFD program ANSYS Airpak, where the Reynolds Average Navier Stokes (RANS) 2-Equation k-ε Renormalization Group (RNG) turbulence model was employed. A very fine, unstructured hexa-mesh of over 450,000

cells was generated and refined near areas of interest, such as the jet discharge and immediately above the sample. Convergence was achieved in approximately 5000 iterations and confirmed by a flattening of the residual curves and velocity monitoring points positioned above the sample. For the high velocity wind tunnel, the wall jet was found to produce a very uniform discharge over the sample and exhibited the characteristic profile for turbulent plane wall jets. An example of the jet profile is presented in Figure 3.7 (side view, plane at the center of the sample). Flow within the multilayer wind tunnel exhibited the classic turbulent duct flow profile.

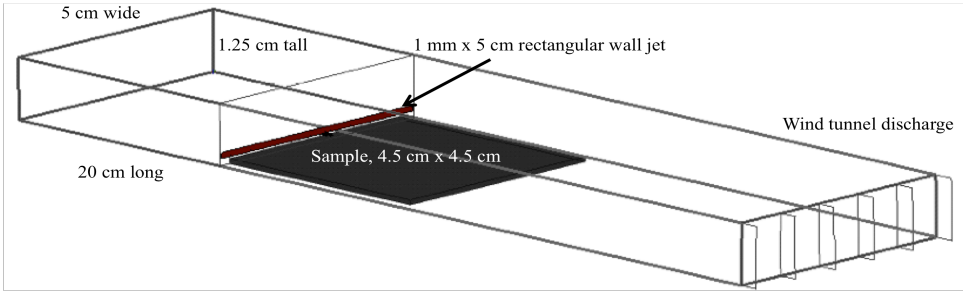

Figure 3.6: ANSYS Airpak model of micro-scale wind tunnel with high velocity wall jet

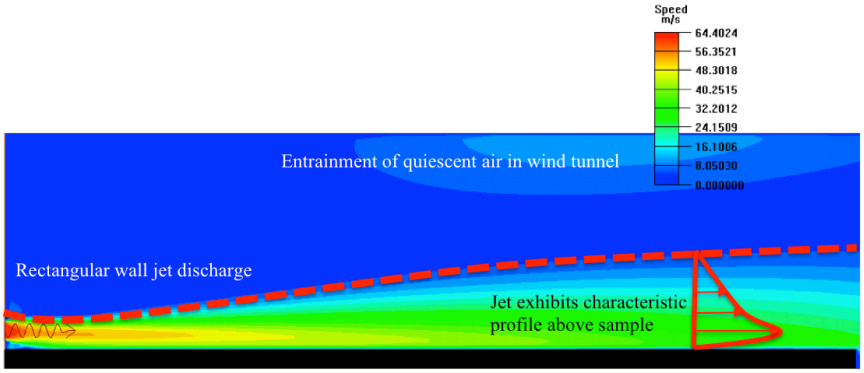

Figure 3.7: Example of CFD velocity contour plot of the turbulent plane wall jet

Air velocity measurements were taken with a one-dimensional constant-temperature hot-wire anemometer, DanTec Dynamics MiniCTA probe 55P16. The

accuracy of the anemometer was limited by the accuracy of the pitot tube/micromanometer used to calibrate the sensor, which was 3%. The anemometer took velocity measurements at a frequency of 1 kHz, which was necessary to capture the turbulent fluctuations of the high velocity wall jet. For the monolayer deposit, three velocities, $\bar{U}$, were studied: 25, 50, and 75 m/s. The running average temporal profiles for each velocity are presented in Figure 3.8 (average over an interval of 0.1 seconds; flow is over galvanized sheet metal in this figure, although there was no noticeable difference in the flow characteristics compared with linoleum). The acceleration of the flow, α, was regulated by the needle valve and was approximately 2 m/s^2 for each of the three velocities. The turbulence intensities, *TI*, were 26.5%, 22.6%, and 21.7% at 25, 50, and 75 m/s, respectively. For the multilayer wind tunnel, the velocities studied were 2.5, 5, 7.5, 10, 12.5, 15, and 25 m/s (profiles not reported here).

The exposure time for both the monolayer and multilayer deposits was 100 seconds. The exposure time can be divided into two temporal regimes: a period of flow acceleration, which was typically less than 30 seconds, depending on the final, steady-state velocity, and period of steady-state flow (example is shown in Figure 3.8). As previously discussed in Chapter 2, resuspension does tend to decay with time, however, this variable was not studied here. A few pilot experiments at low velocities found no significant change in particle resuspension between an exposure time of 10 seconds and 100 seconds, suggesting the majority of resuspension occurs during the acceleration period, similar to the results presented in Ibrahim et al. 2003.

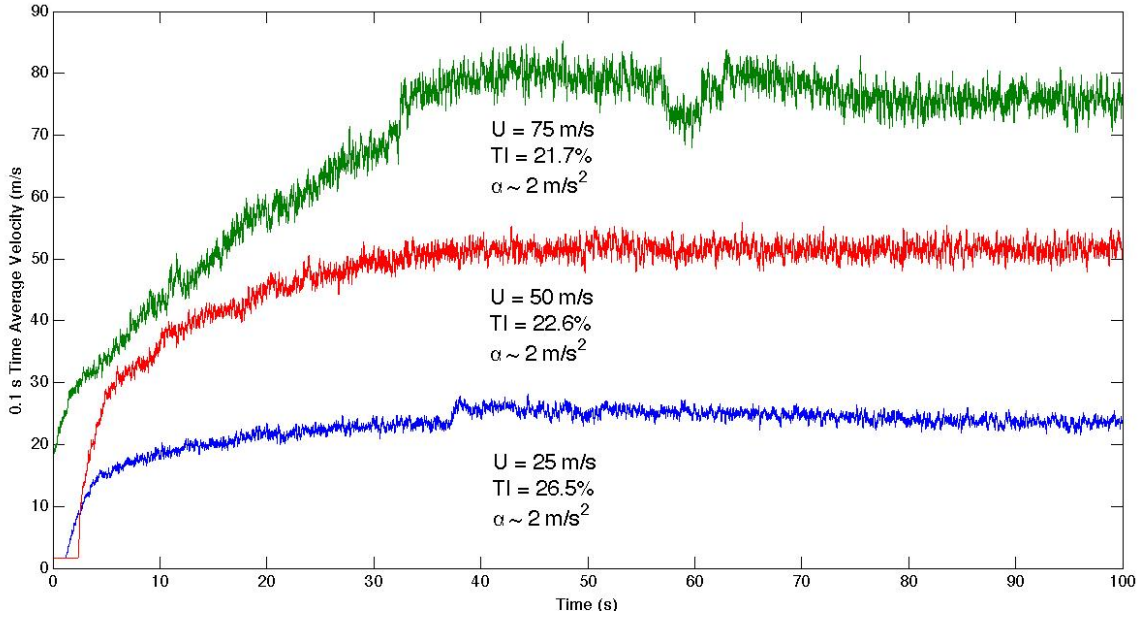

Figure 3.8: Running average velocity profiles over 100 second exposure time

3.5 FLUOROMETRIC METHODS

To determine the absolute resuspension fraction, Φ, for the monolayer particle deposits and the surface and canopy layers of the multilayer deposit, a Leica MZ16FA fluorescence stereomicroscope equipped with a charge-coupled device (CCD) camera was used. The microscope and camera, along with morphometry analysis, were used to determine the seeding density, σ, defined as the number of particles in a given area. The red 3 μm and green 10 μm fluorescent particles were each detected using a different fluorescent filter and microscope and camera settings, as outlined in Table 3.1. The sample was magnified to an appropriate image size via the zoom drive, and brought into focus via the focus drive, both of which were controlled externally. The microscope was equipped with a MultiStep bi-directional scan feature through a motorized X/Y stage control that automatically scans a specified area and compiles the individual images into a larger, mosaic image. This allows a greater fraction of the sample area to be further

analyzed with morphometry software. The exposure time, which is the time that the camera sensing elements are exposed to the sample, gamma (contrast), and gain, which modifies the brilliance of an image, were meticulously modified to obtain images with very high resolution and good contrast between the particle and background surface. As shown in Figures 3.9 and 3.10, a sparse monolayer deposit was verified by ensuring no particle-to-particle contact existed.

Table 3.1: Fluorescence stereomicroscope, camera, and morphometry settings

Particle Diameter	Dye/Filter	Excitation Wavelength	Emission Wavelength	Zoom Drive	Focus Drive	Exposure	Gamma	Gain	Image Area	Image Threshold
3 μm	Red/TXR	542 nm	612 nm	72.5	88-90	0.18-1.2 s	10	10	1.8 mm^2	25
10 μm	Green/GFP3	468 nm	508 nm	10-11	90-91	1.2-1.5 s	10	10	55-80 mm^2	25

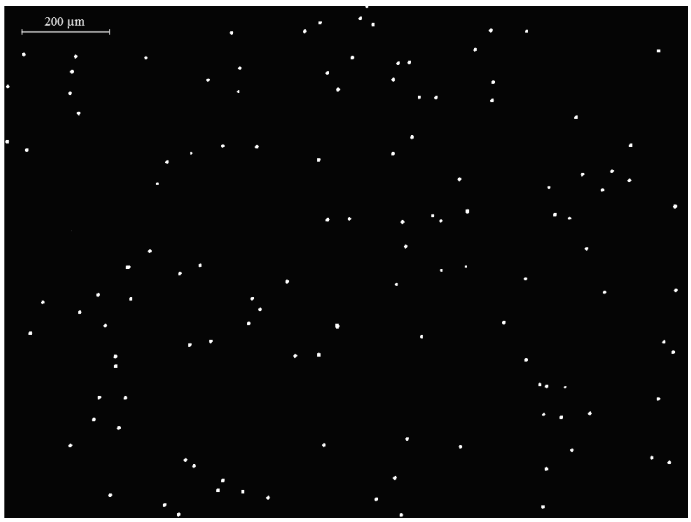

Figure 3.9: Example of fluorescence microscope image: 3 μm particles on galvanized sheet metal. Image size: 1.55 x 1.16 mm.

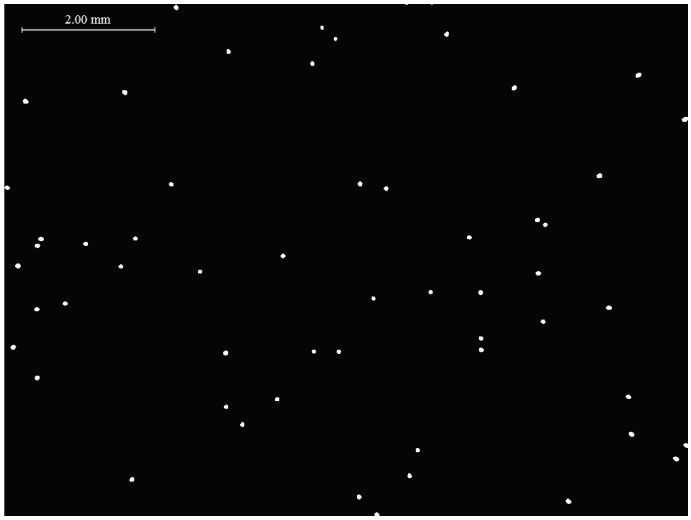

Figure 3.10: Example of fluorescence microscope image: 10 μm particles on galvanized sheet metal. Image size: 10.2 x 7.66 mm.

3.6 MORPHOMETRY ANALYSIS

To count the number of particles within the area of the MultiStep image, and to determine the seeding density, a MATLAB morphometry program was developed (provided in Appendix A.3). The grayscale image produced by the microscope software was converted to a binary image of fully saturated white and black objects through a process known as thresholding. This helps isolate individual white objects, which represent individual particles. A threshold value of 5, on the standard grayscale of 0 to 255, was found to sufficiently isolate particles and remove any background noise produced by the inherent fluorescence of the linoleum, galvanized sheet metal, or ATD in the case of the multilayer deposits. A histogram displaying the area distribution (in pixels^2) was also generated to determine the impact of any outlying objects. As shown in Figure 3.11, the size distribution of 3 μm particles was relatively uniform, with an average area of roughly 50 pixels^2.

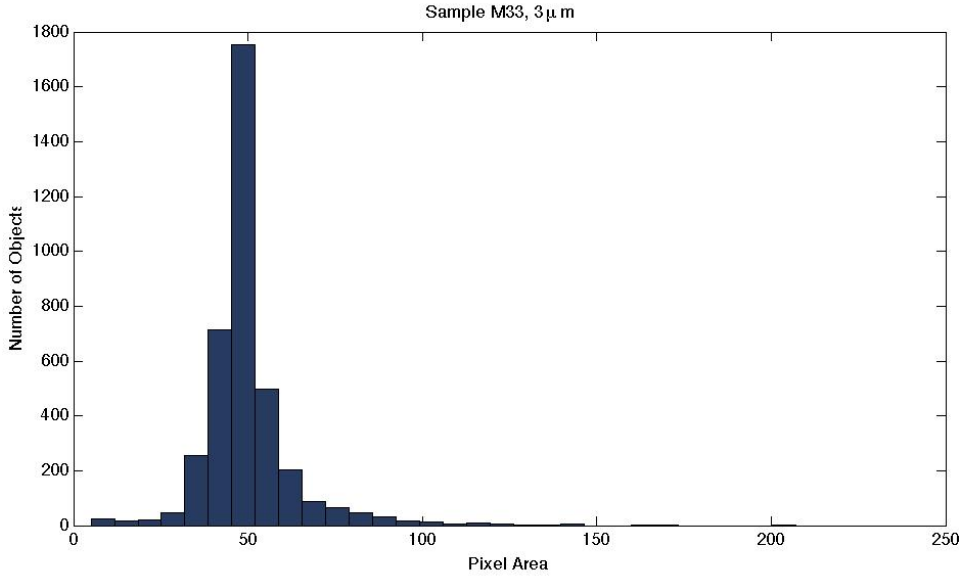

Figure 3.11: Example of 3 μm particle size distribution on a seeded sample

Chapter 4: Preliminary Results & Discussion

Preliminary experiments suggest that particle resuspension from monolayer deposits of 3 and 10 μm particles on linoleum and galvanized sheet metal is very low, even at air velocities as high as 50 m/s. This is in agreement with the monolayer wind tunnel studies of Corn and Stein 1965 and Jiang et al. 2008. However, particle resuspension for the canopy layer of the multilayer particle deposit is significantly higher, and resuspension is even detected at velocities as low as 2.5 m/s. These results demonstrate that when particles are deposited on top of particles, the resulting particle to particle adhesive forces may be less than that between the particle and surface, leading the greater rates of resuspension. This is in agreement with the theoretical work of Israelechvilli 1994 and Lazaridis and Drossinos 1998, which showed that particle-to-particle adhesion is less than that between a particle and a flat surface. Furthermore, it is possible that, because the multilayer deposit extends upward from the surface, the particles deposited along the upper layers are exposed to higher friction velocities than those on the surface layer. This will need to be further investigated by studying the airflow above the surface and through the multilayer deposit, which could be modeled as a porous medium.

4.1 MONOLAYER

Preliminary results for monolayer resuspension experiments are presented in Figures 4.1 and 4.2 (based on 8 samples per case). The findings follow the trend of previous research, including the dependence of resuspension on particle size, air velocity, and relative humidity. The absolute resuspension fraction was found to increase with increasing particle size and air velocity. In addition, resuspension was greater at 35% relative humidity compared to 70% relative humidity. Resuspension was slightly greater

for linoleum compared to galvanized sheet metal, and this could be attributed to the greater surface roughness of linoleum. Lastly, phenomenally high velocities, unrealistic of what would be found indoors, are required to obtain a Φ greater than 0.05.

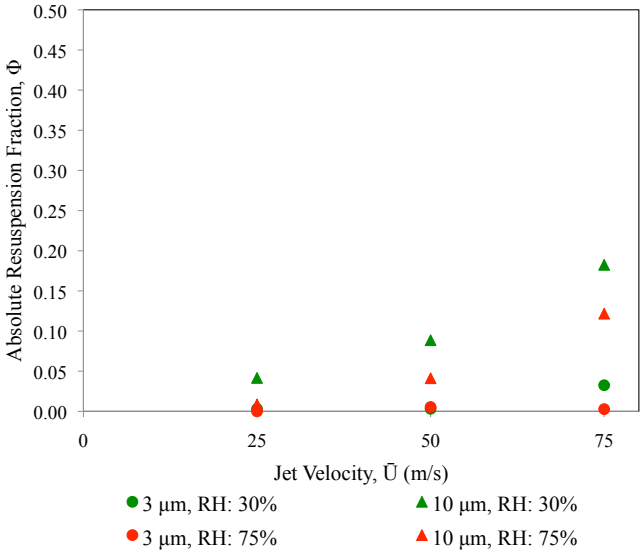

Figure 4.1: Absolute resuspension fractions for a monolayer deposit on galvanized sheet metal

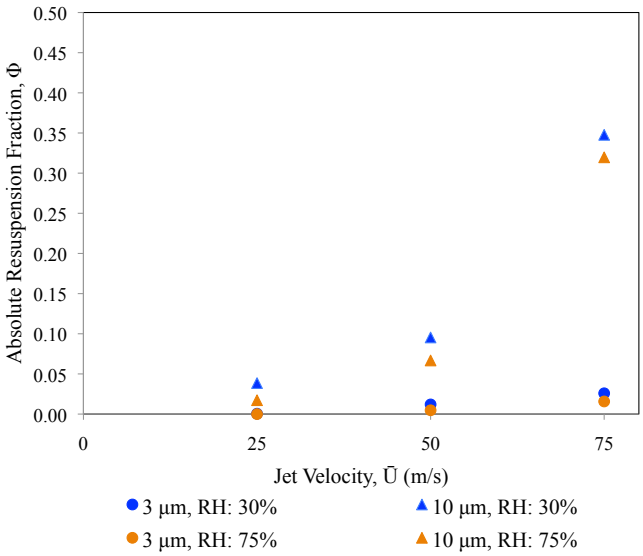

Figure 4.2: Absolute resuspension fractions for a monolayer deposit on linoleum

4.2 MULTILAYER

Absolute resuspension fractions for the canopy (3 μm particles) and surface (10 μm particles) layers of the multilayer deposit with ATD on galvanized sheet metal are reported in Figure 4.3 (based on an average of 2 to 3 samples per case). Resuspension from the canopy layer is found at very low velocities (2.5 and 5 m/s) and Φ surpasses 0.9 at 10 m/s. The surface layer follows the trend of the monolayer deposit results, which show very little resuspension up to 25 m/s. These preliminary results are in agreement with the findings of Lazaridis and Drossinos 1998, who found that the resuspension rate of the surface layer was generally less than that of the outer (canopy) layers because the adhesive force between a particle and a surface is greater than that between two particles. The authors also found that higher friction velocities are necessary to resuspend surface layer particles compared to particles deposited along the outer layers. This follows the trend of the data presented here, in which higher absolute resuspension fractions were found for the canopy layer at lower bulk air velocities (2.5 and 5 m/s, Φ = 0.04 and 0.13, respectively) compared to the resuspension of the sparse surface monolayer deposit at 50 m/s ($\Phi \leq 0.10$).

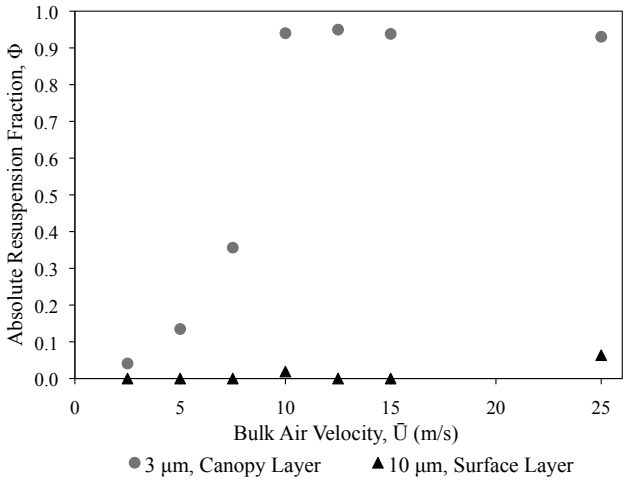

Figure 4.3: Absolute resuspension fractions for a multilayer deposit on galvanized sheet metal

Chapter 5: Conclusion & Future Work

This paper provides a literature review of monolayer and multilayer particle resuspension and presents an experimental method to determine resuspension from both types of deposits on indoor surfaces. Some of the important variables that impact resuspension include: particle size, air velocity, relative humidity, surface characteristics, material properties, and characteristics of the airflow. In addition, there are several distinctions between monolayer and multilayer deposits: resuspension of the upper layers of multilayer deposits can occur at much lower air velocities compared to monolayer deposits and particles will tend to resuspend in the form of large clusters from multilayer deposits. It is likely that particle deposits in the indoor environment fall somewhere between a monolayer and multilayer, so it is important to understand how resuspension differs between the two.

The experimental methodology presented in this paper provides a systematic means to investigate particle resuspension from the two types of deposits from indoor surfaces under a variety of environmental conditions. Preliminary results confirm the findings of previous research. Particle resuspension was found to be significantly greater for multilayer deposits compared to monolayer deposits. This suggests that resuspension, and subsequently inhalation exposure, may be greater for heavy dust loads that can accumulate on surfaces in the indoor environment. This research is presently ongoing and will be extended to investigate the structure of particle deposits in the indoor environment and how variables, such as thickness and porosity, affect particle resuspension. To do so, various microscopy techniques, including scanning electron microscopy (SEM), will be employed.

Appendix

A.1 Particle Counter Matlab Code

```
%Particle Counter

clc
close all

%Enter file name & image dimensions
I=imread('File_Name.tif');

%Enter image size (mm)
x=10.2;
y=7.66;

%Enter multi-Step a x b
a=2;
b=4;

%Display image
imshow(I);
figure, imhist(I);

%Threshold image
level=graythresh(I);
bw=im2bw(I,level);
bw=bwareaopen(bw, 5);
imshow(bw);

%Identify objects (particles)
ob=bwconncomp(bw);

%Calculate seeding density
sd=ob.NumObjects/(a*b*x*y);

%Size distribution of particles
obdata=regionprops(ob,'basic');
ob_area=[obdata.Area];
nbins=30;
figure, hist(ob_area,nbins);
```

References

Ahmadi, G. & Guo, S. Bumpy particle adhesion and removal in turbulent flows including electrostatic and capillary forces. *The Journal of Adhesion* **83**, 289-311(2007).

Ahmadi, G., Guo, S. & Zhang, X. Particle adhesion and detachment in turbulent flows including capillary forces. *Particulate Science and Technology* **25**, 59-76(2007).

Bagnold, R.A. *The Physics of Blown Sand and Desert Dunes*. Methuen London & Co. Ltd., London(1941).

Batterman, S.A. & Burge, H. HVAC systems as emission sources affecting indoor air quality: a critical review. *HVAC&R Research* **1**, 61–80(1996).

Bejan, A. Convection heat transfer. John Wiley & Sons, Inc., New Jersey(2004).

Biasi, L., de los Reyes, A., Reeks, M.W. & de Santi, G.F.. Use of a simple model for the interpretation of experimental data on particle resuspension in turbulent flows. *Journal of Aerosol Science* **32**, 1175-1200(2001).

Braaten, D. A, Paw U, K.T. & Shaw, R.H. Particle resuspension in a turbulent boundary layer-observed and modeled. *Journal of Aerosol Science* **21**, 613-628(1990).

Braaten, D. A. Wind tunnel experiments of large particle reentrainment-deposition and development of large particle scaling parameters. *Aerosol Science and Technology* **21**, 157-169(1994).

Callister, W.D. Materials science and engineering: an introduction. John Wiley & Sons, Inc., New York(2007).

Chiou, S.F. & Tsai, C.J. Measurement of emission factor of road dust in a wind tunnel. *Powder Technology* **118**, 10-15(2001).

Cleaver, J. S. & Looi, L. AFM study of adhesion between polystyrene particles: the influence of relative humidity and applied load. *Powder Technology* **174**, 34-37(2007).

Cleaver, J. & Yates, B. Mechanism of detachment of colloidal particles from a flat substrate in a turbulent flow. *Journal of Colloid and Interface Science* **44**, 464–474(1973).

Corn, M. The adhesion of solid particles to solid surfaces. *Journal of Air Pollution Control Association* **11**, 566-575(1961).

Corn, M. & Stein, F. Re-entrainment of particles from a plane surface. *American Industrial Hygiene Association Journal* **26**, 325-336(1965).

El Hamdani, S., Limam, K., Abadie, M.O. & Bendou, A. Deposition of fine particles on building internal surfaces. *Atmospheric Environment* **42**, 8893-8901(2008).

Ferro, A., Kopperud, R. & Hildemann, L. Source strengths for indoor human activities that resuspend particulate matter. *Environmental Science & Technology* **38**, 1759-64(2004).

Friess, H. & Yadigaroglu, G. A generic model for the resuspension of multilayer aerosol deposits by turbulent flow. *Nuclear science and engineering* **138**, 161–176(2001).

Friess, H. & Yadigaroglu, G. Modelling of the resuspension of particle clusters from multilayer aerosol deposits with variable porosity. *Journal of Aerosol Science* **33**, 883-906(2002).

Fromentin, A. Time dependent particle resuspension from a multi-layer deposit by turbulent flow. *Journal of Aerosol Science* **20**, 911-914(1989).

Gac, J., Sosnowski, T. & Gradon, L. Turbulent flow energy for aerosolization of powder particles. *Journal of Aerosol Science* **39**, 113-126(2008).

Gomes, C., Freihaut, J. & Bahnfleth, W. Resuspension of allergen-containing particles under mechanical and aerodynamic disturbances from human walking. *Atmospheric Environment* **41**, 5257-5270(2007).

Greenwood, J. & Williamson, J. Contact of nominally flat surfaces. *Proceeding of the Royal Society A* **295**, 300-319(1966).

Guingo, M. & Minier, J. A new model for the simulation of particle resuspension by turbulent flows based on a stochastic description of wall roughness and adhesion forces. *Journal of Aerosol Science* **39**, 957-973(2008).

Hall, D. The time dependence of particle resuspension. *Journal of Aerosol Science* **20**, 907-910(1989).

Hall, D. & Reed, J. The time dependence of the resuspension of particles. *Journal of Aerosol Science* **20**, 839–842(1989).

Hays, D.A. Electric field detachment of toner. *Photography Science and Engineering* **22**, 232-235(1978).

Hinds, W.C. Aerosol technology: properties, behavior, and measurement of airborne particles. John Wiley & Sons, Inc., New York(1999).

Hu, B., Freihaut, J.D., Bahnfleth, W.P. & Thran, B.. Measurements and factorial analysis of micron-sized particle adhesion aorce to indoor flooring materials by electrostatic detachment method. *Aerosol Science and Technology* **42**, 513-520(2008).

Ibrahim, A.H., Ghosh, S. & Dunn, P.F. Detachment of tobacco-smoke-material carriers from surfaces by turbulent air flow. *Journal of Environmental Monitoring* **11**, 56-62(2009).

Ibrahim, A.H. & Dunn, P. Effects of temporal flow acceleration on the detachment of microparticles from surfaces. *Journal of Aerosol Science* **37**, 1258-1266(2006).

Ibrahim, A.H, Dunn, P. & Brach, R. Microparticle detachment from surfaces exposed to turbulent air flow: controlled experiments and modeling. *Journal of Aerosol Science* **34**, 765-782(2003).

Ibrahim, A.H., Dunn, P. & Brach, R. Microparticle detachment from surfaces exposed to turbulent air flow: effects of flow and particle deposition characteristics. *Journal of Aerosol Science* **35**, 805-821(2004).

Ibrahim, A.H., Dunn, P. & Qazi, M. Experiments and validation of a model for microparticle detachment from a surface by turbulent air flow. *Journal of Aerosol Science* **39**, 645-656(2008).

Israelachvilli, J. Intermolecular and surface forces, Academic Press, New York(1994).

Jiang, Y., Matsusaka, S., Masuda, H. & Qian, Y. Characterizing the effect of substrate surface roughness on particle–wall interaction with the airflow method. *Powder Technology* **186**, 199-205(2008).

Johnson, K.L., Kendall, K. & Roberts, A.D. Surface energy and the contact of elastic solid. *Proceedings of the Royal Society of London, Series A, Mathematical and Physical Sciences* **324**, 301-313(1971).

Jurcik, B. & Wang, H.C. The modelling of particle resuspension in turbulent flow. *Journal of Aerosol Science* **22**, S149–S152(1991).

Kim, Y., Gidwani, A., Wyslouzil, B.E. & Sohn, C.W. Source term models for fine particle resuspension from indoor surfaces. *Building and Environment* **45**, 1854-1865(2010).

Klepeis, N.E., Nelson, W.C., Ott, W.R., Robinson, J.P., Tsang, A.M., Switzer, P., Behar, J.V., Hern, S.C & Engelmann, W.H. The National Human Activity Pattern Survey (NHAPS): a resource for assessing exposure to environmental pollutants. *Journal of Exposure Analysis and Environmental Epidemiology* **11**, 231-52(2001).

Krauter, P. & Biermann, A. Reaerosolization of fluidized spores in ventilation systems. *Applied and Environmental Microbiology* **73**, 2165-72(2007).

Laden, F., Neas, L.M., Dockery, D.W. & Schwartz, J.. Association of fine particulate matter from different sources with daily mortality in six U.S. cities. *Environmental Health Perspectives* **108**, 941-7(2000).

Lazaridis, M. & Drossinos, Y. Resuspension of small particles by turbulent flow. *Journal of Aerosol Science* **26**, S579-S580(1995).

Lazaridis, M., Drossinos, Y. & Georgopoulos, P. Turbulent resuspension of small nondeformable particles. *Journal of Colloid and Interface Science* **204**, 24-32(1998).

Lazaridis, M. & Drossinos, Y. Multilayer resuspension of small identical particles by turbulent flow. *Aerosol Science and Technology* **28**, 548-560(1998).

Leighton, D. & Acrivos, A. The lift on a small sphere touching a plane in the presence of a simple shear flow. *Zeitschrift fur Angewandte Mathematik und Physik* **36**, 174-178(1985).

Lohaus, J.H. Adhesion of particles on indoor flooring materials. Ph.D. Dissertation, The University of Texas at Austin(2007).

Lohaus, J.H., Novoselac, A. & Siegel, J.A. Particle resuspension from indoor flooring materials. *Proceedings of the 11th International Conference on Indoor Air and Climate*, paper ID 342,1(2008).

Matsusaka, S. & Masuda, H. Particle reentrainment from a fine powder layer in a turbulent air flow. *Aerosol Science and Technology* **24**, 69-84(1996).

Miguel, A.F., Aydin, M. & Heitor Reis, A. Indoor deposition and forced re-suspension of respirable particles. *Indoor and Built Environment* **14**, 391-396(2005).

Montoya, L. & Hildemann, L. Size distributions and height variations of airborne particulate matter and cat allergen indoors immediately following dust-disturbing activities. *Journal of Aerosol Science* **36**, 735-749(2005).

Mukai, C., Siegel, J.A. & Novoselac, A. Impact of airflow characteristics on particle resuspension from indoor surfaces. *Aerosol Science and Technology* **43**, 1022-1032(2009).

Muller, V.M., Yushchenko, V.S. & Derjaguin, B.V. On the influence of molecular forces on the deformation of an elastic sphere and its sticking to a rigid plane. *Journal of Colloid and Interface Science* **77**, 91-101(1980).

Nazaroff, W.W. Indoor particle dynamics. *Indoor Air* **14**, 175-83(2004).

Nicholson, K. A review of particle resuspension. *Atmospheric Environment* **22**, 1069-77(1988).

Nicholson, K. Wind tunnel experiments on the resuspension of particulate material. *Atmospheric Environment. Part A. General Topics* **27**, 181–188(1993).

Nitschke, D. & Schmidt, E. A new approach to model the re-entrainment of settled particles based on film theory of fluid mass transfer processes. *Particle & Particle Systems Characterization* **26**, 58-68(2009).

O'Meara, T. & Tovey, E. Monitoring personal allergen exposure. *Clinical reviews in Allergy & Immunology* **18**, 341-95(2000).

O'Neill, M. A sphere in contact with a plane in a slow shear linear flow. *Chemical Engineering Science* **23**, 1293-1298(1968).

Ostro, B.D., Hurley, S. & Lipsett, M.J. Air pollution and daily mortality in the Coachella Valley, California: a study of PM10 dominated by coarse particles. *Environmental Research* **81**, 231-8(1999).

Ott, W.R., Steinemann, A.C. & Wallace, L.A. Exposure analysis. Taylor & Francis Group, Boca Raton, Florida(2007).

Paajanen, M., Katainen, J., Pakarinen, O.H., Foster, A.S. & Lahtinen, J. Experimental humidity dependency of small particle adhesion on silica and titania. *Journal of Colloid and Interface Science* **304**, 518-23(2006).

Pakarinen, O.H., Foster, A.S., Paajanen, M., Kalinainen, T., Katainen, J., Makkonen, I., Lahtinen, J. & Nieminen, R.M. Towards an accurate description of the capillary

force in nanoparticle-surface interactions. *Modelling and Simulation in Materials Science and Engineering* **13**, 1175-1186(2005).

Peters, A., Liu, E., Verrier, R.L., Schwartz, J., Gold, D.R., Mittleman, M., Baliff, J., Oh, J.A., Allen, G., Monahan, K. & Dockery, D.W. Air pollution and incidence of cardiac arrhythmia. *Epidemiology* **11**, 11-17(2000).

Polichetti, G., Cocco, S., Spinali, A., Trimarco, V. & Nunziata, A. Effects of particulate matter (PM(10), PM(2.5) and PM(1)) on the cardiovascular system. *Toxicology* **261**, 1-8(2009).

Pope, C.A., Verrier, R.L., Lovett, E.G., Larson, A.C., Raizenne, M.E., Kanner, R.E., Schwartz, J., Villegas, G.M, Gold, D.R. & Dockery, D.W. Heart rate variability associated with particulate air pollution. *American Heart Journal* **138**, 890-9(1999).

Qian, J. & Ferro, A. Resuspension of dust particles in a chamber and associated environmental factors. *Aerosol Science and Technology* **42**, 566-578(2008).

Reeks, M. & Hall, D. Kinetic models for particle resuspension in turbulent flows: theory and measurement. *Journal of Aerosol Science* **32**, 1-31(2001).

Reeks, M., Reed, J. & Hall, D. On the resuspension of small particles by a turbulent flow. *Journal of Physics D: Applied Physics* **21**, 574(1988).

Rim, D. & Novoselac, A. Transport of particulate and gaseous pollutants in the vicinity of a human body. *Building and Environment* **44**, 1840-1849(2009).

Rosati, J., Thornburg, J. & Rodes, C. Resuspension of particulate matter from carpet due to human activity. *Aerosol Science and Technology* **42**, 472-482(2008).

Sehmel, G. Particle resuspension: a review. *Environment International* **4**, 107–127(1980).

Sippola, M. & Nazaroff, W.W. Experiments measuring particle deposition from fully developed turbulent flow in ventilation ducts. *Aerosol Science and Technology* **38**, 914-925(2004).

Soltani, M. & Ahmadi, G. On particle adhesion and removal mechanisms in turbulent flows. *Journal of Adhesion Science and Technology* **8**, 763-785(1994).

Soltani, M. & Ahmadi, G. Direct numerical channel flow simulation of particle entrainment in turbulent channel flow. *Physics of Fluids* **7**, 647-657(1995).

Souza, M.B., Saldiva, P.H.N., Pope, C.A. & Capelozzi, V.L. Respiratory changes due to long-term exposure to urban levels of air pollution. *Chest* **113**, 1312(1998).

Swanson, M.C., Agarwal, M.K. & Reed, C.E. An immunochemical approach to indoor aeroallergen quantitation with a new volumetric air sampler: studies with mite, roach, cat, mouse, and guinea pig antigens. *Journal of Allergy and Clinical Immunology* **76**, 724-729(1985).

Tadmor, J. & Zur, I. Resuspension of particles from a horizontal surface. *Atmospheric Environment* **15**, 141-149(1981).

Thatcher, T.L. & Layton, D.W. Deposition, resuspension, and penetration of particles within a residence. *Atmospheric Environment* **29**, 1487-1497(1995).

Tsai, C.-J., Pui, D.Y.H. & Liu, B.Y.H. Elastic flattening and particle adhesion. *Aerosol Science and Technology* **15**, 239-255(1991).

U.S. Environmental Protection Agency. PM Standards Revision – 2006. Available: http://www.epa.gov/pm/naaqsrev2006.html. Accessed 21 October 2010.

Wallace, L.A. Indoor particles: a review. *Journal of Air and Waste Management Association* **46**, 98-126(1996).

Wen, H. & Kasper, G. On the kinetics of particle reentrainment from surfaces. *Journal of Aerosol Science* **20**, 483-498(1989).

Wu, Y.-L., Davidson, C.I. & Russell, A.G. Controlled wind tunnel experiments for particle bounceoff and resuspension. *Aerosol Science and Technology* **17**, 245-262(1992).

Zimon, A.D. Adhesion of dust and powder, 2nd ed., Consultants Bureau, New York, pp. 307-319(1982).

Ziskind, G. Particle resuspension from surfaces: revisited and re-evaluated. *Reviews in Chemical Engineering* **22**, 1-123(2006).

Ziskind, G., Yarin, L.P., Peles, S. & Gutfinger, C. Experimental investigation of particle removal from surfaces by pulsed air jets. *Aerosol Science & Technology* **36**, 652-659(2002).

Ziskind, G., Fichman, M. & Gutfinger, C. Resuspension of particulates from surfaces to turbulent flows–Review and analysis. *Journal of Aerosol Science* **26**, 613–644(1995).

Vita

Brandon Boor was born in Smithtown, New York in 1987 to Lila and Brian Boor. He grew up in Columbia, Maryland, where he attended Long Reach High School and participated in the Howard County Technology Magnet Program. He studied Mechanical Engineering at York College of Pennsylvania and graduated summa cum laude with a Bachelors of Science degree in August 2009. That same month, he began graduate studies at The University of Texas at Austin as a M.S./Ph.D. student in the Environmental and Water Resources Engineering program. He was awarded a National Science Foundation Graduate Research Fellowship in April 2010.

Permanent address: 8162 Tamar Drive, Columbia, MD 21045, brandoneboor@gmail.com
This thesis was typed by Brandon Emil Boor